Received: 18 August 2023 | Revised: 6 March 2024 | Accepted: 21 March 2024

DOI: 10.1002/nme.7496

RESEARCH ARTICLE

WILEY

Identification of dominant subspaces for model reduction of structured parametric systems

Peter Benner | **Pawan Goyal** | **Igor Pontes Duff**

Max Planck Institute for Dynamics of Complex Technical Systems, Magdeburg, Germany

Correspondence
Igor Pontes Duff, Max Planck Institute for Dynamics of Complex Technical Systems, Sandtorstraße 1, Magdeburg 39106, Germany.
Email: pontes@mpi-magdeburg.mpg.de

Summary

In this paper, we discuss a novel model reduction framework for linear structured dynamical systems. The transfer functions of these systems are assumed to have a special structure, for example, coming from second-order linear systems or time-delay systems, and they may also have parameter dependencies. Firstly, we investigate the connection between classic interpolation-based model reduction methods with the reachability and observability subspaces of linear structured parametric systems. We show that if enough interpolation points are taken, the projection matrices of interpolation-based model reduction encode these subspaces. Consequently, we are able to identify the dominant reachable and observable subspaces of the underlying system. Based on this, we propose a new model reduction algorithm combining these features and leading to reduced-order systems. Furthermore, we discuss computational aspects of the approach and its applicability to a large-scale setting. We illustrate the efficiency of the proposed approach with several numerical large-scale benchmark examples.

KEYWORDS

controllability and observability, interpolation, linear structured systems, model order reduction, parametric systems

1 | INTRODUCTION

In this paper, we consider linear structured parametric systems, having transfer functions of the form:

$$\mathbf{H}(s,\mathbf{p}) = \mathcal{C}(s,\mathbf{p})\mathcal{K}(s,\mathbf{p})^{-1}\mathcal{B}(s,\mathbf{p}), \tag{1}$$

where

$$\mathcal{C}(s,\mathbf{p}) = \sum_{i=1}^{k}\gamma_i(s,\mathbf{p})\mathbf{C}_i, \quad \mathcal{K}(s,\mathbf{p}) = \sum_{i=1}^{l}\kappa_i(s,\mathbf{p})\mathbf{A}_i, \quad \mathcal{B}(s,\mathbf{p}) = \sum_{i=1}^{q}\beta_i(s,\mathbf{p})\mathbf{B}_i, \tag{2}$$

in which $\mathbf{A}_i \in \mathbb{R}^{n\times n}$, $\mathbf{B}_i \in \mathbb{R}^{n\times m}$, $\mathbf{C}_i \in \mathbb{R}^{p\times n}$ are constant matrices, s takes values in $\mathbb{C}$, and $\mathbf{p} = \left[p^{(1)}, \ldots, p^{(d)}\right] \in \Omega^d$ are the system parameters. $\kappa_i(s,\mathbf{p})$, $\beta_i(s,\mathbf{p})$ and $\gamma_i(s,\mathbf{p})$ are functions of $s \in \mathbb{C}$ and $\mathbf{p} \in \Omega^d$. Additionally, the restrictions

$\kappa_i(\cdot,\mathbf{p})$, $\beta_i(\cdot,\mathbf{p})$ and $\gamma_i(\cdot,\mathbf{p})$ are assumed to be meromorphic functions. The assumption of meromorphic coefficients will be used to ensure that (1) is well-defined, that is, that the inverse $\mathcal{K}(s,\mathbf{p})^{-1}$ exists almost everywhere (in the sense that the set of poles of K(s,p) forms a set of Lebesgue measure zero). The system (1) covers a large class of linear systems, arising in various science and engineering applications, for example, classical linear systems, second-order systems, time-delay systems, integro-differential systems, and their parameter-dependent variants.

In order to illustrate the class of systems (1), we consider a dynamical system arising in computational electro-magnetics presented in Reference 1. A discretized system can be obtained by the spatial discretization of the electromagnetic field equations, describing the electro-dynamical behavior of microwave devices when the surface losses are included in the physical model. The transfer function of the system has a very particular structure; precisely, it has a fractional integrator and takes the form:

$$\mathbf{H}(s) = \sqrt{s}\mathbf{B}^\top\left(s^2\mathbf{I} - \frac{1}{\sqrt{s}}\mathbf{D} + \mathbf{A}\right)^{-1}\sqrt{s}\mathbf{B}. \tag{3}$$

If the above equation is compared with the form given in Equation (1) for a fixed parameter, then the matrices $\mathcal{C}(s)$, $\mathcal{K}(s)$ and $\mathcal{B}(s)$ can be given by

$$\mathcal{C}(s) = \sqrt{s}\mathbf{B}^\top, \quad \mathcal{K}(s) = \left(s^2\mathbf{I} - \frac{1}{\sqrt{s}}\mathbf{D} + \mathbf{A}\right), \qquad \mathcal{B}(s) = \sqrt{s}\mathbf{B},$$

and

$$\gamma_1(s) = \beta_1(s) = \sqrt{s}, \quad \kappa_1(s) = s^2, \quad \kappa_2(s) = -\frac{1}{\sqrt{s}}, \quad \kappa_3(s) \equiv 1,$$
$$\mathbf{B}_1 = \mathbf{C}_1^\top = \mathbf{B}, \quad \mathbf{A}_1 = \mathbf{I}, \quad \mathbf{A}_2 = \mathbf{D}, \quad \text{and} \quad \mathbf{A}_3 = \mathbf{A}.$$

Hence, the transfer function (3) fits into our framework (1).

Model order reduction (MOR) has been studied extensively in the literature for some classes of linear systems, see, for example, References 2,3 for standard linear systems,[4–7] for second-order systems,[8,9] for time-delay systems, and the review paper[10] for parametric systems. Furthermore, several researchers have investigated MOR techniques for the generalized linear systems (1). For a fixed parameter, balanced truncation has been proposed in Reference 11. The method requires computing the system Gramians, namely reachability and observability Gramians, which can be a computationally challenging task in a large-scale setting. Another popular MOR method, transfer function interpolation, has also been studied,[12,13] where for a given set of interpolation points, it is shown how to construct an interpolating reduced-order system while preserving the system structure. However, References 12,13 leave an important open problem about the choice of a good set of interpolation points. Furthermore, we would like to mention that a data-driven approach for structured non-parametric systems has been studied in Reference 14. Nevertheless, the construction of the structured reduced-order system is not a straightforward task; more importantly, it is not clear how to construct a reachable and observable system. It is worth noticing that for parametric non structured systems, the authors in Reference 15 have developed optimization-based methods for the $\mathcal{H}_2 \otimes \mathcal{L}_2$ error. Although the approach has new developments on the optimality conditions, its implementation is still numerically expensive for medium to large scale systems.

In this paper, we discuss a connection between interpolation-based MOR methods with the reachable and observable subspaces of linear structured parametric systems. We show that if enough interpolation points are taken, the projection matrices of interpolation-based model reduction encode these subspaces. As a consequence, we propose an approach to construct reduced-order systems preserving the common subspaces containing the most reachable as well as the most observable states. This approach can be seen as a combination of the interpolation-based method in Reference 12, and of some aspects of the Loewner framework for first-order systems.[16]

The precise structure of the paper is as follows. In the subsequent section, we discuss the construction of interpolating reduced-order systems for (1) for a given set of interpolation points s and parameters $\mathbf{p}$. Thereafter, in Section 3, we define the concepts of reachability and observability for linear structured parametric systems and connect them with interpolation-based MOR methods. Subsequently, by combining both features, we discuss the construction of reduced-order systems keeping the subspaces of the most reachable and observable states simultaneously. In Section 5,

we illustrate the efficiency of the approach using several benchmark examples and finally conclude with future avenues. In the rest of the paper, we make use of the following notation.

- $\texttt{svd}\{\cdot\}$ denotes the singular value decomposition (SVD) of a matrix.
- By using MATLAB® notation, we denote the first l columns of a matrix $\mathbf{V}$ by $\mathbf{V}(:, 1:l)$.
- Let $\mathcal{V}$ be a subspace of $\mathbb{C}^n$ (or $\mathbb{R}^n$). We denote the orthogonal complement of $\mathcal{V}$ by $\mathcal{V}^\perp$.
- Let $\mathbf{H}(\cdot)$ and $\mathbf{G}(\cdot)$ be two matrix valued complex functions. We say that $\mathbf{H}(s) \overset{a.e.}{=} \mathbf{G}(s)$ if $\mathbf{H}(s) = \mathbf{G}(s)$ for almost every $s \in \mathbb{C}$.

2 | PRELIMINARY WORK

In this section, we briefly recap the interpolatory framework to construct reduced-order systems from Reference 12. Let us consider linear systems whose input-output mappings (transfer functions) are given in (1). Our goal is to construct reduced-order systems, having a similar structure using Petrov-Galerkin projection as follows:

$$\widehat{\mathbf{H}}(s, \mathbf{p}) = \widehat{\mathcal{C}}(s, \mathbf{p})\widehat{\mathcal{K}}(s, \mathbf{p})^{-1}\widehat{\mathcal{B}}(s, \mathbf{p}), \tag{4}$$

where

$$\widehat{\mathcal{C}}(s, \mathbf{p}) = \mathcal{C}(s, \mathbf{p})\mathbf{V}, \qquad \widehat{\mathcal{K}}(s, \mathbf{p}) = \mathbf{W}^\top\mathcal{K}(s, \mathbf{p})\mathbf{V}, \qquad \widehat{\mathcal{B}}(s, \mathbf{p}) = \mathbf{W}^\top\mathcal{B}(s, \mathbf{p}). \tag{5}$$

We aim at determining full-rank matrices $\mathbf{V}$ and $\mathbf{W}$ in a way that the resulting reduced-order system interpolates a given set of interpolation points for s and $\mathbf{p}$. This problem was considered in Reference 12, where the idea of constructing interpolatory non-parametric structured systems[13] and classical linear parametric systems[17] was extended to the systems (4). However, the authors in Reference 12 present the framework for linear structured parametric systems, where the functions given in (2) can be decomposed as $q(s, \mathbf{p}) := q_s(s)q_p(\mathbf{p})$, but this can be readily extended to the general case. In the following theorem, we present a variation of this result where this decomposition is not required.

Theorem 1. *Let $\mathbf{H}(s, \mathbf{p})$ be a transfer function as in (1). Consider interpolation points $\{\sigma_i, \mathbf{p}_i\}$ and $\{\mu_i, \mathbf{q}_i\}$, $i \in \{1, \dots, r\}$, such that $\mathcal{K}(s, \mathbf{p})$ is invertible for $\{s, \mathbf{p}\} \in \{\sigma_i, \mathbf{p}_i\} \cup \{\mu_i, \mathbf{q}_i\}$. Furthermore, let the full-rank matrices $\mathbf{V}, \mathbf{W} \in \mathbb{C}^{n\times r}$ satisfy*:

$$\operatorname*{span}_{i\in\{1,\dots,r\}} \left\{\mathcal{K}(\sigma_i, \mathbf{p}_i)^{-1}\mathcal{B}(\sigma_i, \mathbf{p}_i)\right\} \subseteq \operatorname{range}(\mathbf{V}), \tag{6a}$$

$$\operatorname*{span}_{i\in\{1,\dots,r\}} \left\{\mathcal{K}(\mu_i, \mathbf{q}_i)^{-\top}\mathcal{C}(\mu_i, \mathbf{q}_i)^\top\right\} \subseteq \operatorname{range}(\mathbf{W}). \tag{6b}$$

If the reduced matrices are computed as shown in (5), then the following conditions are satisfied, for $i \in \{1, \dots, r\}$:

$$\mathbf{H}(\sigma_i, \mathbf{p}_i) = \widehat{\mathbf{H}}(\sigma_i, \mathbf{p}_i), \tag{7a}$$

$$\mathbf{H}(\mu_i, \mathbf{q}_i) = \widehat{\mathbf{H}}(\mu_i, \mathbf{q}_i). \tag{7b}$$

Moreover, if $\mu_i = \sigma_i$, $\mathbf{q}_i = \mathbf{p}_i$ for $i \in \{1, \dots, r\}$, and $\mathbf{H}(s, \mathbf{p})$ and $\widehat{\mathbf{H}}(s, \mathbf{p})$ are differentiable at $(\sigma_i, \mathbf{p}_i)$ for $i \in \{1, \dots, r\}$, then along with (7a,b), the following conditions are satisfied:

$$\frac{d}{ds}\mathbf{H}(\sigma_i, \mathbf{p}_i) = \frac{d}{ds}\widehat{\mathbf{H}}(\sigma_i, \mathbf{p}_i), \tag{8a}$$

$$\nabla_{\mathbf{p}}\mathbf{H}(\sigma_i, \mathbf{p}_i) = \nabla_{\mathbf{p}}\widehat{\mathbf{H}}(\sigma_i, \mathbf{p}_i). \tag{8b}$$

Proof. The theorem can be proven exactly along the lines given in Reference 12. We begin by proving (7a). We have

$$\begin{aligned}\widehat{\mathbf{H}}(\sigma_i,\mathbf{p}_i) &= \widehat{\mathcal{C}}(\sigma_i,\mathbf{p}_i)\widehat{\mathcal{K}}(\sigma_i,\mathbf{p}_i)^{-1}\widehat{\mathcal{B}}(\sigma_i,\mathbf{p}_i)\\ &= \mathcal{C}(\sigma_i,\mathbf{p}_i)\mathbf{V}\widehat{\mathcal{K}}(\sigma_i,\mathbf{p}_i)^{-1}\mathbf{W}^\top\mathcal{B}(\sigma_i,\mathbf{p}_i)\\ &= \mathcal{C}(\sigma_i,\mathbf{p}_i)\mathbf{V}\widehat{\mathcal{K}}(\sigma_i,\mathbf{p}_i)^{-1}\mathbf{W}^\top\mathcal{K}(\sigma_i,\mathbf{p}_i)\underbrace{\mathcal{K}(\sigma_i,\mathbf{p}_i)^{-1}\mathcal{B}(\sigma_i,\mathbf{p}_i)}_{\in\operatorname{range}(\mathbf{V})}\\ &= \mathcal{C}(\sigma_i,\mathbf{p}_i)\mathbf{V}\widehat{\mathcal{K}}(\sigma_i,\mathbf{p}_i)^{-1}\mathbf{W}^\top\mathcal{K}(\sigma_i,\mathbf{p}_i)\mathbf{V}z\\ &= \mathcal{C}(\sigma_i,\mathbf{p}_i)\mathbf{V}z = \mathcal{C}(\sigma_i,\mathbf{p}_i)\mathcal{K}(\sigma_i,\mathbf{p}_i)^{-1}\mathcal{B}(\sigma_i,\mathbf{p}_i) = \mathbf{H}(\sigma_i,\mathbf{p}_i).\end{aligned}$$

Analogously, we can prove (7b). Furthermore, we can prove (8a) and (8b) along the lines given in References 13 and 17, respectively. For the sake of brevity, we refrain from providing a complete proof. ∎

In the previous theorem, we have seen how an interpolatory reduced-order system can be constructed for a given set of interpolation points. However, a good choice of interpolation points for both frequency (s) and the parameters ($\mathbf{p}$) is essential to construct a good reduced-order system. Additionally, the problem of finding suitable candidates for interpolation points does not have a straightforward answer. Therefore, in this work, we take a different approach. Precisely, we show that given a sufficiently large number of interpolation points, we can determine the important subspaces, leading to good quality of the reduced-order systems. To that end, we first discuss the concepts of reachability and observability for dynamical systems.

3 | REACHABILITY, OBSERVABILITY, AND REDUCED-ORDER SYSTEMS

This section aims at showing the connection of the Petrov-Galerkin projection matrices $\mathbf{V}$ and $\mathbf{W}$ in (6a,b) (Theorem 1) with the classical concepts of reachability and observability of dynamical systems. Based on this, we can identify the states that are simultaneously least reachable and least observable. This leads to an algorithm which is a combination of interpolation and SVD techniques, enabling us to construct reduced-order systems for structured parametric systems. We begin here by briefly revisiting some results for first-order linear systems.

3.1 | Background on first-order systems

The transfer function of a first-order system is given by

$$\mathbf{H}_{\mathrm{fo}}(s) = \mathbf{C}(s\mathbf{I}-\mathbf{A})^{-1}\mathbf{B}, \quad \text{with } \mathbf{A}\in\mathbb{C}^{n\times n},\ \mathbf{B}\in\mathbb{C}^{n\times m} \text{ and } \mathbf{C}\in\mathbb{C}^{p\times n}. \tag{9}$$

We note that the reachable subspace $\mathcal{V}_R$ and the observable subspace $\mathcal{W}_O$ of the system (9) are given by the smallest subspaces of $\mathbb{C}^n$ such that

$$\operatorname{range}\left(e^{\mathbf{A}t}\mathbf{B}\right)\subset\mathcal{V}_R \quad \text{and} \quad \operatorname{range}\left(e^{\mathbf{A}^\top t}\mathbf{C}^\top\right)\subset\mathcal{W}_O \ \text{ for every } t\geq 0.$$

This essentially follows from standard proofs relating reachability and observability of linear-time invariant systems with the rank of the Kalman reachability and observability matrices defined as follows:

$$\mathbf{M}_R(\mathbf{A},\mathbf{B}) = \begin{bmatrix}\mathbf{B} & \mathbf{A}\mathbf{B} & \mathbf{A}^2\mathbf{B} & \dots & \mathbf{A}^{n-1}\mathbf{B}\end{bmatrix}, \text{ and} \tag{10a}$$

$$\mathbf{M}_O^\top(\mathbf{C},\mathbf{A}) = \begin{bmatrix}\mathbf{C}^\top & \mathbf{A}^\top\mathbf{C}^\top & (\mathbf{A}^2)^\top\mathbf{C}^\top & \dots & (\mathbf{A}^{n-1})^\top\mathbf{C}^\top\end{bmatrix}, \tag{10b}$$

see Reference 18, chap. 2 for more details. The unreachable subspace, which is the orthogonal complement of $\mathcal{V}_R$ and denoted by $\mathcal{V}_R^\perp$, consists of the states $\mathbf{q}_{ur}\in\mathbb{C}^n$ such that $\mathbf{q}_{ur}^\top e^{\mathbf{A}t}\mathbf{B}=0$ for every $t\geq 0$. Similarly, the unobservable

subspace, characterized by $\mathcal{W}_O^{\perp}$, consists of the states $\mathbf{q}_{uo} \in \mathbb{C}^n$ such that $\mathbf{C}e^{\mathbf{A}t}\mathbf{q}_{uo} = 0$ for every $t \geq 0$. By means of the Laplace transform, the reachability and observability subspaces can be seen as the smallest subspaces of $\mathbb{C}^n$ such that

$$\operatorname{range}\big((s\mathbf{I}-\mathbf{A})^{-1}\mathbf{B}\big) \subset \mathcal{V}_R, \quad \text{and} \quad \operatorname{range}\big((s\mathbf{I}-\mathbf{A})^{-\top}\mathbf{C}^{\top}\big) \subset \mathcal{W}_O, \quad \forall s \in i\mathbb{R}. \tag{11}$$

Additionally, we note that the system (9) is reachable if $\mathcal{V}_R = \mathbb{C}^n$, and observable if $\mathcal{W}_O = \mathbb{C}^n$. A classical result in system theory is that if the system (9) is not reachable or not observable, then there exists a system of lower order, having the same transfer function as the original one. Indeed, the unreachable or unobservable states, denoted by $\mathcal{V}_R^{\perp}$ and $\mathcal{W}_O^{\perp}$, respectively, can be removed from the dynamics, without changing the transfer function. Moreover, if the system is reachable and observable, then it is minimal, that is, there exists no lower-order realization for the original transfer function, see, for example, Reference 18, chap. 2.

For first-order systems, a well-known characterization of reachable and observable spaces is given by $\mathcal{V}_R = \operatorname{range}(\mathbf{M}_R(\mathbf{A},\mathbf{B}))$ and $\mathcal{W}_O = \operatorname{range}\big(\mathbf{M}_O^{\top}(\mathbf{C},\mathbf{A})\big)$, where $\mathbf{M}_R(\mathbf{A},\mathbf{B})$ and $\mathbf{M}_O^{\top}(\mathbf{C},\mathbf{A})$ are, respectively, the Kalman reachability and observability matrices given in (10a,b). Furthermore, the authors in Reference 19 provided a different characterization of these subspaces which is closely related to the interpolation problem. In particular, they have shown that $\mathcal{V}_R = \operatorname{range}(\mathbf{V})$ and $\mathcal{W}_O = \operatorname{range}(\mathbf{W})$, where

$$\mathbf{V} = \Big[(\sigma_1\mathbf{I}-\mathbf{A})^{-1}\mathbf{B}, (\sigma_2\mathbf{I}-\mathbf{A})^{-1}\mathbf{B}, \ \dots\ , (\sigma_N\mathbf{I}-\mathbf{A})^{-1}\mathbf{B}\Big], \text{ and}$$
$$\mathbf{W} = \Big[(\sigma_1\mathbf{I}-\mathbf{A})^{-\top}\mathbf{C}^{\top}, (\sigma_2\mathbf{I}-\mathbf{A})^{-\top}\mathbf{C}^{\top}, \ \dots\ , (\sigma_N\mathbf{I}-\mathbf{A})^{-\top}\mathbf{C}^{\top}\Big]$$

with $N \geq n$ and $\sigma_k \in i\mathbb{R}$ not an eigenvalue of $\mathbf{A}$, $k \in \{1, \dots, N\}$, are distinct points. Notice that the above matrices $\mathbf{V}$ and $\mathbf{W}$ are the particular matrices $\mathbf{V}$ and $\mathbf{W}$ from Theorem 1 when the original system is first-order non-parametric. Moreover, also in Reference 19 and more recently in Reference 16, the authors have shown that the matrix $\begin{bmatrix}\mathbf{W}^{\top}\mathbf{V} & \mathbf{W}^{\top}\mathbf{A}\mathbf{V}\end{bmatrix}$ encodes the dimension of the minimal order realization of the original system, that is,

$$\operatorname{rank}\left(\begin{bmatrix}\mathbf{W}^{\top}\mathbf{V} & \mathbf{W}^{\top}\mathbf{A}\mathbf{V}\end{bmatrix}\right) := \begin{cases}\text{order of the minimal realization obtained by}\\ \text{removing unreachable and unobservable states}\end{cases}$$

Furthermore, in Reference 16, an algorithm based on the SVD is provided in order to get the minimal realization or reduced-order systems by Petrov-Galerkin projections.

Inspired by the above discussion on first-order systems, in what follows, we first extend some of the results to linear structured systems (1), and propose an algorithm, allowing us to construct reduced-order systems by removing unreachable and unobservable subspaces.

3.2 | Reachability, observability, and reduced systems for linear structured systems

As mentioned earlier, unreachable or unobservable states can be removed from first-order systems (9) such that the resulting lower-order system has the same transfer function as the original one. In this section, we study how these notions can be extended to the class of structured systems (1). For the clarity of exposition, we start our discussion with the non-parametric case, that is, linear structured systems of the form

$$\mathbf{H}(s) = \mathcal{C}(s)\mathcal{K}(s)^{-1}\mathcal{B}(s). \tag{12}$$

Dynamical systems can be represented using different frameworks, for example, as a semi-group in a Hilbert space, as a linear system over a ring of operators and as a functional differential equation. Depending on the nature of representation or the considered problem, there exist various definitions for reachability and observability.

For the infinite-dimensional control community, dynamical systems are represented in the infinite-dimensional setting, where the state-space might be seen as an (infinite-dimensional) Hilbert space associated with a semi-group. There, the notions of exact and approximate reachability and observability play an important role, see, for example, References 20,21 and 22, chap. 4. However, in this setup, the dynamical systems are no longer seen as functional differential equations.

Hence, discretizing the infinite-dimensional Hilbert space leads to finite-dimensional first-order reduced-order systems that do not preserve the structure in (12).

Another point of view is the one in algebraic system theory, which considers dynamical systems as linear systems over a ring, see, for example, References 23,24. In this setting, the reachability and observability concepts rely on a rank condition over a ring, for example, strong and weak reachability/observability, see References 25–27. However, since these concepts depend on the underlying ring, we are not aware of a way to adapt it to a structure-preserving reduction in the Petrov-Galerkin projection framework.

In this paper, we define a weaker notion of reachability/observability that relies only on linear algebra concepts and the matrices of the realization of the system (12). These concepts are related to the realization of the transfer function (12) as a functional differential equation, see References 11,28. To begin our discussion, we first make the following assumption on the structure of (12):

Assumption 1. In (12), we assume $\mathcal{K}(s)$ to have the following form:

$$\mathcal{K}(s) = \alpha_1(s)\mathbf{A}_1 + \sum_{i=2}^{l} \alpha_i(s)\mathbf{A}_i,$$

and, furthermore, that the following conditions are satisfied:

1. $\mathbf{A}_1$ is non-singular,
2. $\dfrac{\alpha_k(\imath\omega)}{\alpha_1(\imath\omega)} \to 0$ as $|\omega| \to \infty$, $\omega \in \mathbb{R}$, and $k \in \{2, \ldots, l\}$.

Assumption 1 states that the first meromorphic function $\alpha_1(s)$ dominates the others at infinity. Additionally, its corresponding matrix $\mathbf{A}_1$ is assumed to be nonsingular. Under this assumption, the following result holds.

Proposition 1. *Under Assumption 1, the generalized pencil $\mathcal{K}(s)$ is regular, that is,*

$$f(s) = \det \mathcal{K}(s) \not\equiv 0.$$

Moreover, since f is a nonzero meromorphic function, it has a countable number of zeros, and $\mathcal{K}(s)$ is invertible almost everywhere in $\mathbb{C}$.

Proof. We note that

$$\begin{aligned} f(s) = \det \mathcal{K}(s) &= \det\left(\alpha_1(s)\left(\mathbf{A}_1 + \sum_{i=2}^{l} \frac{\alpha_i(s)}{\alpha_1(s)}\mathbf{A}_i\right)\right) \\ &= \alpha_1(s)^n \det\left(\mathbf{A}_1 + \sum_{i=2}^{l} \frac{\alpha_i(s)}{\alpha_1(s)}\mathbf{A}_i\right). \end{aligned}$$

Due to $\frac{\alpha_i(\imath\omega)}{\alpha_1(\imath\omega)} \to 0$ as $|\omega| \to \infty$, $f(\imath\omega)$ is asymptotically equivalent to $\alpha_1(\imath\omega)^n \det(\mathbf{A}_1)$. As a consequence, since $\mathbf{A}_1$ is non-singular, $f(s)$ cannot be the zero function. The rest of the result follows from the fact that $f(s)$ is meromorphic. ∎

From now on, in this section, we assume that $\mathcal{K}(s)$ satisfies Assumption 1. Next, we define the reachability/observability notions relevant to this work.

Definition 1. The $\mathbb{C}^n$–reachable subspace $\mathcal{V}_R$ associated to the pair of functions $(\mathcal{K}(s), \mathcal{B}(s))$ is the smallest subspace of $\mathbb{C}^n$ which contains $\operatorname{range}\left(\mathcal{K}(s)^{-1}\mathcal{B}(s)\right)$ for all $s \in i\mathbb{R}$. In other words, if $\mathcal{V}_R = \operatorname{range}(\mathbf{V}_R)$, where $\mathbf{V}_R \in \mathbb{C}^{n\times r_R}$ is a full column rank matrix and $r_R \le n$, we have

$$\mathcal{K}(s)^{-1}\mathcal{B}(s) = \mathbf{V}_R y_R(s), \tag{13}$$

in which $y_R(s) \in \mathbb{C}^{r_R\times m}$ is a matrix of meromorphic functions. In this case, we say that $(\mathcal{K}(s), \mathcal{B}(s))$ is $\mathbb{C}^n$–*reachable* if $\mathcal{V}_R = \mathbb{C}^n$.

The $\mathbb{C}^n$–*unreachable subspace* consists of the states $\mathbf{q}_{ur} \in \mathbb{C}^n$ such that

$$\mathbf{q}_{ur}^{\top}\mathcal{K}(s)^{-1}\mathcal{B}(s) = 0 \quad \forall s \in i\mathbb{R}.$$

As a consequence, the $\mathbb{C}^n$–unreachable subspace is characterized by $\mathcal{V}_R^{\perp}$. It is worth noting that, in the case of first-order systems (9), that is, $\mathcal{K}(s)^{-1}\mathcal{B}(s) = (s\mathbf{I} - \mathbf{A})^{-1}\mathbf{B}$, the above definition generalizes (11).

We now recall that the transfer from the input to the state for system (12) is given by

$$\mathbf{x}(s) = \mathcal{K}(s)^{-1}\mathcal{B}(s)\mathbf{u}(s).$$

Hence, the $\mathbb{C}^n$–reachable subspace $\mathcal{V}_R$ corresponds to the smallest subspace that contains the states $\mathbf{x}(s)$ for every s and input function $\mathbf{u}(s)$. This justifies the use of the reachability terminology.

To connect the frequency and time-domains, let $\mathbf{M}(t)$ denote the inverse Laplace transform of $\mathcal{K}(s)^{-1}\mathcal{B}(s)$. Hence, by definition $\mathbf{M}(t) = \mathbf{V}_R\mathbf{Y}(t)\ \forall t \geq 0$, where $\mathbf{Y}(t)$ is the inverse Laplace transform of $y_R(s)$ in (13). It can be noticed that, for real systems, that is, systems where $\mathbf{M}(t)$ is a real function, the matrix $\mathbf{V}_R$ can be chosen as a real matrix. Also, in the context of time-delay systems, Definition 1 is equivalent to the one of point-wise complete controllability, see References 29,30 and of $\mathbb{R}^n$–controllability,[23] chap. 2. Similarly, we use the following concept of observability.

Definition 2. The $\mathbb{C}^n$–observable subspace $\mathcal{W}_O$ associated to the pair of functions $(\mathcal{C}(s), \mathcal{K}(s))$ is the smallest subspace of $\mathbb{C}^n$ which contains range$\left(\mathcal{K}(s)^{-\top}\mathcal{C}(s)^{\top}\right)$, for all $s \in i\mathbb{R}$. In other words, if $\mathcal{W}_O = \text{range}(\mathbf{W}_O)$, where $\mathbf{W}_O \in \mathbb{C}^{n\times r_O}$ is a full-rank matrix and $r_O \leq n$, we have

$$\mathcal{C}(s)\mathcal{K}(s)^{-1} = y_O(s)\mathbf{W}_O^{\top},$$

in which $y_O(s) \in \mathbb{C}^{p\times r_O}$ is a matrix of meromorphic functions. In this case, we say that $(\mathcal{C}(s), \mathcal{K}(s))$ is $\mathbb{C}^n$–*observable* if $\mathcal{W}_O = \mathbb{C}^n$.

The $\mathbb{C}^n$–*unobservable subspace* consists of the states $\mathbf{q}_{uo} \in \mathbb{C}^n$ such that

$$\mathcal{C}(s)\mathcal{K}(s)^{-1}\mathbf{q}_{uo} = 0 \quad \forall s \in i\mathbb{R},$$

and thus is characterized by $\mathcal{W}_O^{\perp}$. Similarly, in the case of first-order systems, that is, (9), $\mathcal{K}(s)^{-\top}\mathcal{C}^{\top}(s) = (s\mathbf{I} - \mathbf{A})^{-\top}\mathbf{C}^{\top}$ and the above definition is a natural extension of (11) for observability. As discussed for the $\mathbb{C}^n$ reachability space, $\mathbf{W}_O$ can be chosen to be real if the original system represents real dynamics.

Analogous to first-order systems (9), if a structured system (12) is not $\mathbb{C}^n$–reachable or $\mathbb{C}^n$–observable, then there exists a lower-order system that has the same transfer function. We state the result rigorously in the following theorem.

Theorem 2. *Let $(\mathcal{C}(s), \mathcal{K}(s), \mathcal{B}(s))$ be a linear structured system of order n as shown in (12). If either $(\mathcal{C}(s), \mathcal{K}(s))$ is not $\mathbb{C}^n$–observable or $(\mathcal{K}(s), \mathcal{B}(s))$ is not $\mathbb{C}^n$–reachable, then there exists a lower-order structured realization $(\widehat{\mathcal{C}}(s), \widehat{\mathcal{K}}(s), \widehat{\mathcal{B}}(s))$ of order $r < n$, realizing the original transfer function, that is,*

$$\mathcal{C}(s)\mathcal{K}(s)^{-1}\mathcal{B}(s) \overset{a.e.}{=} \widehat{\mathcal{C}}(s)\widehat{\mathcal{K}}(s)^{-1}\widehat{\mathcal{B}}(s).$$

Proof. Let us first consider the case where the structured system is not $\mathbb{C}^n$–reachable. In this case, there exist $r_R < n$ and a full-rank matrix $\mathbf{V}_R \in \mathbb{C}^{n\times r_R}$ such that $\mathcal{K}(s)^{-1}\mathcal{B}(s) = \mathbf{V}_R\mathcal{Z}(s)$. From Assumption 1, there exists a matrix $\mathbf{W} \in \mathbb{R}^{n\times r_R}$ such that $\mathbf{W}^{\top}\mathbf{A}_1\mathbf{V}_R$ is non-singular. As a consequence, the projected generalized pencil

$$\widehat{\mathcal{K}}(s) = \alpha_1(s)\mathbf{W}^{\top}\mathbf{A}_1\mathbf{V}_R + \sum_{i=2}^{l}\alpha_i(s)\mathbf{W}^{\top}\mathbf{A}_i\mathbf{V}_R$$

also satisfies Assumption 1. Hence, from Proposition 1, $\widehat{\mathcal{K}}(s)$ is invertible almost everywhere in $\mathbb{C}$. Therefore, $(\mathbf{W}^{\top}\mathcal{K}(s)\mathbf{V}_R)^{-1}\mathbf{W}^{\top}\mathcal{B}(s) = \widehat{\mathcal{K}}(s)^{-1}\mathbf{W}^{\top}\mathcal{B}(s) \overset{a.e.}{=} \mathcal{Z}(s)$ and we have

$$\mathcal{K}(s)^{-1}\mathcal{B}(s) \overset{a.e.}{=} \mathbf{V}_R(\mathbf{W}^\top\mathcal{K}(s)\mathbf{V}_R)^{-1}\mathbf{W}^\top\mathcal{B}(s). \tag{14}$$

Thus,

$$\mathcal{C}(s)\mathcal{K}(s)^{-1}\mathcal{B}(s) \overset{a.e.}{=} \widehat{\mathcal{C}}(s)\widehat{\mathcal{K}}(s)^{-1}\widehat{\mathcal{B}}(s)$$

with

$$\widehat{\mathcal{C}}(s) = \mathcal{C}(s)\mathbf{V}_R \in \mathbb{C}^{p\times r}, \quad \widehat{\mathcal{K}}(s) = \mathbf{W}^\top\mathcal{K}(s)\mathbf{V}_R \in \mathbb{C}^{r\times r}, \quad \text{and} \quad \widehat{\mathcal{B}}(s) = \mathbf{W}^\top\mathcal{B}(s) \in \mathbb{C}^{r\times m}.$$

Similarly, when the system is not $\mathbb{C}^n$–observable, it can be shown that there exists a lower-order realization■

The above result states that if a structured realization is not $\mathbb{C}^n$–reachable or not $\mathbb{C}^n$–observable, then there exists a lower-order structured realization which represents the same transfer function. Moreover, a lower-order realization can be obtained via Petrov-Galerkin projection.

Remark 1. The counterpart of Theorem 2 is valid for first-order systems (9), that is, if the first order system (9) is reachable and observable, then the system is minimal. Until now we have not been able to find a concrete hypothesis for this result to hold for more general structured systems. For the current set up, the following counter example holds. Consider the structured system given by

$$\mathcal{K}(s) = \begin{bmatrix} s+1 & & \\ & s+2 & \\ & & s+3 \end{bmatrix}, \quad \mathcal{B}(s) = \begin{bmatrix} 1 \\ 1 \\ (s+3) \end{bmatrix}, \quad \text{and} \quad \mathcal{C}(s) = \begin{bmatrix} 1 & -(s+2) & 1 \end{bmatrix}.$$

The $\mathbb{C}^n$–reachable subspace $\mathbf{V}_R$ is the smallest subspace, containing $\mathcal{K}(s)^{-1}\mathcal{B}(s) = \begin{bmatrix} \frac{1}{s+1} \\ \frac{1}{s+2} \\ 1 \end{bmatrix}$ for every $s \in i\mathbb{R}$. Hence, $\mathcal{V}_R = \mathbb{C}^3$ and the system is $\mathbb{C}^n$–reachable. In a similar way, one can show that the system is $\mathbb{C}^n$–observable. However, the transfer function is $\mathbf{H}(s) = \mathcal{C}(s)\mathcal{K}(s)^{-1}\mathcal{B}(s) = \frac{1}{s+1}$ and, hence the realization is not minimal. As a conclusion, for general structured systems, $\mathbb{C}^n$–reachability and $\mathbb{C}^n$–observability are not enough to characterize minimality.

However, it is worth noticing that the above example can be transformed into an equivalent system by means of the following transformation:

$$\widetilde{\mathcal{K}}(s) = \mathbf{U}_1(s)\overline{\mathcal{K}}(s)\mathbf{U}_2(s) = \begin{bmatrix} s+1 & & \\ & 1 & \\ & & 1 \end{bmatrix}, \quad \widetilde{\mathcal{B}}(s) = \mathbf{U}_1(s)\mathcal{B}(s) = \begin{bmatrix} 1 \\ 1 \\ 1 \end{bmatrix}, \quad \text{and}$$
$$\widetilde{\mathcal{C}}(s) = \mathcal{C}(s)\mathbf{U}_2(s) = \begin{bmatrix} 1 & -1 & 1 \end{bmatrix},$$

where $\mathbf{U}_1(s) = \operatorname{diag}\left(1, 1, \frac{1}{s+3}\right)$ and $\mathbf{U}_2(s) = \operatorname{diag}\left(1, \frac{1}{s+2}, 1\right)$. For the transformed system, one can easily find that the $\mathbb{C}^n$–reachable subspace $\mathcal{V}_R = \operatorname{range}\left(\begin{bmatrix} 1 & 0 \\ 0 & 1 \\ 0 & 1 \end{bmatrix}\right)$ and the $\mathbb{C}^n$–observable subspace $\mathcal{W}_O = \operatorname{range}\left(\begin{bmatrix} 1 & 0 \\ 0 & -1 \\ 0 & 1 \end{bmatrix}\right)$. As a consequence, for this equivalent realization, the system is not $\mathbb{C}^n$–reachable and $\mathbb{C}^n$–observable and hence the minimal realization $\mathbf{H}(s) = \frac{1}{s+1}$ can be constructed be removing the subspaces that are not reachable and not observable. Hence, for the transformed realization $\widetilde{\mathcal{K}}(s)$, $\widetilde{\mathcal{B}}(s)$ and $\widetilde{\mathcal{C}}(s)$, we are able to construct the minimal realization only based on $\mathbb{C}^n$–reachability and $\mathbb{C}^n$–observability properties. In other words, the way $\mathcal{K}(s)$, $\mathcal{B}(s)$ and $\mathcal{C}(s)$ are modeled might play an important role in the search for the

minimal realization of structured systems using the $\mathbb{C}^n$–reachable and $\mathbb{C}^n$–observable subspaces. However, an investigation on additional conditions required for minimality is out of the scope of this work.

We have shown that if we know reachable and observable subspaces $\mathcal{V}_R$ and $\mathcal{W}_O$, we are able to construct lower-order systems by removing the states that are unreachable or unobservable. The next step is to characterize these spaces using matrices $\mathbf{V}$ and $\mathbf{W}$ defined in Theorem 1. By definition, it is easy to observe that range($\mathbf{V}$) $\subseteq \mathcal{V}_R$ and range($\mathbf{W}$) $\subseteq \mathcal{W}_O$. Additionally, there always exist $N \in \mathbb{N}$ and interpolation points $\sigma_1, \ldots, \sigma_N$ such that

$$\mathbf{V} = \left[\mathcal{K}(\sigma_1)^{-1}\mathcal{B}(\sigma_1), \mathcal{K}(\sigma_2)^{-1}\mathcal{B}(\sigma_2), \ldots, \mathcal{K}(\sigma_N)^{-1}\mathcal{B}(\sigma_N)\right], \tag{15a}$$

$$\mathbf{W} = \left[\mathcal{K}(\sigma_1)^{-\top}\mathcal{C}(\sigma_1)^{\top}, \mathcal{K}(\sigma_2)^{-\top}\mathcal{C}(\sigma_2)^{\top}, \ldots, \mathcal{K}(\sigma_N)^{-\top}\mathcal{C}(\sigma_N)^{\top}\right], \tag{15b}$$

and

$$\text{range}(\mathbf{V}) = \mathcal{V}_R \quad \text{and} \quad \text{range}(\mathbf{W}) = \mathcal{W}_O.$$

Moreover, the above proposition shows that we might only need r interpolation points to characterize the subspaces $\mathcal{V}_R$ and $\mathcal{W}_O$.

Proposition 2. *Suppose that* $\dim(\mathcal{V}_R) = r$. *Then, for* $N \geq r$ *and*

$$\mathbf{V} = \left[\mathcal{K}(\sigma_1)^{-1}\mathcal{B}(\sigma_1), \mathcal{K}(\sigma_2)^{-1}\mathcal{B}(\sigma_2), \ldots, \mathcal{K}(\sigma_N)^{-1}\mathcal{B}(\sigma_N)\right],$$

it holds that range($\mathbf{V}$) $= \mathcal{V}_R$, *for almost every selection of* $\sigma_1, \ldots, \sigma_N$.

Proof. Suppose that range($\mathbf{V}$) $\neq \mathcal{V}_R$ for the selection of points $\sigma_1, \ldots, \sigma_N$. Since range($\mathbf{V}$) $\subset \mathcal{V}_R$, there exists $\mathbf{w} \in \mathcal{V}_R$ such that $\mathbf{w} \perp$ range($\mathbf{V}$), that is, $\mathbf{w}^T\mathbf{V} = 0$. As a consequence, $\mathbf{w}^T\mathcal{K}(\sigma_k)^{-1}\mathbf{B}(\sigma_k) = 0$ for $k = 1, \ldots, N$. Hence, σ_k are the zeros of the meromorphic function $\mathbf{f}(s) = \mathbf{w}^T\mathcal{K}(s)^{-1}\mathbf{B}(s)$. Since $\mathbf{f}(s)$ has a countable number of zeros, this proves the result. ∎

Proposition 2 states that if we know that the dimension of the reachability subspace $\mathcal{V}_R$ is r, then we just need to compute $\mathcal{K}(\sigma_i)^{-1}\mathcal{B}(\sigma_i)$ for r different interpolation points to characterize this subspace. As consequence, if we have enough interpolation points, that is, more than r, we can characterize this subspace. It is worth mentioning that the dimension of the reachability subspace r is not known a priori and it is problem dependent. Throughout this manuscript, we will use the expression "enough interpolation points" with the meaning that the number of points is more than r for the underlying problem.

The above result can be straightforwardly extended to the characterization of the subspace $\mathcal{W}_O$ using the matrix $\mathbf{W}$. Moreover, an immediate consequence of Proposition 2 is that the matrix $\mathbf{V}$ has rank r for almost every selection of N different interpolation points. Additionally, we would like to mention that the matrix $\mathbf{V}$ (likewise the matrix $\mathbf{W}$) can be interpreted as snapshots in frequency domain taken at various frequency points. Therefore, more snapshots would lead to a better subspace that encodes the reachability subspace. It is worth mentioning that, according to Proposition 2, those snapshots could be selected in any place of the frequency domain, even in the same neighborhood. However, in practice, the choice of snapshots in the same neighborhood is not ideal, because they would provide very similar subspace information, often rendering the columns of $\mathbf{V}$ or $\mathbf{W}$ almost linearly dependent.

3.3 | Note on the parametric case

So far, we have presented the definitions of $\mathbb{C}^n$-reachability and $\mathbb{C}^n$-observability for structured non-parametric systems. For the parametric case (1), we can consider the following natural extensions of Definitions 1 and 2. The reachable subspace $\mathcal{V}_R = \text{range}(\mathbf{V}_R)$ associated to the pair of functions $(\mathcal{K}(s,\mathbf{p}), \mathcal{B}(s,\mathbf{p}))$, with a full column rank matrix $\mathbf{V}_R \in \mathbb{C}^{n\times r_R}$, $r_R \leq n$, is the smallest subspace of $\mathbb{C}^n$ which contains $\mathcal{K}(s,\mathbf{p})^{-1}\mathcal{B}(s,\mathbf{p})$ for every $s \in i\mathbb{R}$ and $\mathbf{p} \in \Omega^d$. In other words,

$$\mathcal{K}(s,\mathbf{p})^{-1}\mathcal{B}(s,\mathbf{p}) = \mathbf{V}_R\mathbf{z}_c(s,\mathbf{p}),$$

where $\mathbf{z}_c(s,\mathbf{p}) \in \mathbb{C}^{p\times r_R}$. Similarly, the $\mathbb{C}^n$–observable subspace $\mathcal{W}_O = \text{range}(\mathbf{W}_O)$ associated to $(\mathcal{C}(s,\mathbf{p}), \mathcal{K}(s,\mathbf{p}))$, with a full-rank matrix $\mathbf{W}_O \in \mathbb{C}^{n\times r_O}$, $r_O \le n$, is the smallest subspace of $\mathbb{C}^n$ which contains $\mathcal{K}(s,\mathbf{p})^{-\top}\mathcal{C}(s,\mathbf{p})^\top$ for every $s \in \mathbb{C}$ and $\mathbf{p} \in \Omega^d$. In other words,

$$\mathcal{C}(s,\mathbf{p})\mathcal{K}(s,\mathbf{p})^{-1} = y_O(s,\mathbf{p})\mathbf{W}_O,$$

where $y_O(s,\mathbf{p}) \in \mathbb{C}^{p\times r_O}$ is a matrix of meromorphic functions. Furthermore, the result of Theorem 2 can be extended to the parametric case, showing that states that are unreachable and unobservable can be removed. Additionally, we know that if we take enough interpolation points $(\sigma_i, \mathbf{p}_i)$, the matrices

$$\mathbf{V} = \left[\mathcal{K}(\sigma_1,\mathbf{p}_1)^{-1}\mathcal{B}(\sigma_1,\mathbf{p}_1),\ \dots\ ,\mathcal{K}(\sigma_N,\mathbf{p}_N)^{-1}\mathcal{B}(\sigma_N,\mathbf{p}_{N)}\right], \tag{16a}$$

$$\mathbf{W} = \left[\mathcal{K}(\sigma_1,\mathbf{p}_1)^{-\top}\mathcal{C}(\sigma_1,\mathbf{p}_1)^\top,\ \dots\ ,\mathcal{K}(\sigma_N,\mathbf{p}_N)^{-\top}\mathcal{C}(\sigma_N,\mathbf{p}_N)^\top\right], \tag{16b}$$

encode the reachability and observability spaces, that is,

$$\text{range}(\mathbf{V}) = \mathcal{V}_R \quad \text{and} \quad \text{range}(\mathbf{W}) = \mathcal{W}_O.$$

From now on, we assume that we have enough interpolation points such that $\text{range}(\mathbf{V}) = \mathcal{V}_R$ and $\text{range}(\mathbf{W}) = \mathcal{W}_O$. Although in theory, the nonparametric and parametric cases have a very similar structure, in practice, for parametric examples, the identification of dominant subspaces might require a large amount of samples, which can be impractical in some cases (see Reference 10).

3.4 | Simultaneous reduction

We have seen that if the system (1) is not $\mathbb{C}^n$–reachable or not $\mathbb{C}^n$–observable, there exists a lower-order realization whose transfer function remains the same as the original one. To obtain such a lower-order realization, one needs to truncate the states that are unreachable or unobservable, as shown in Theorem 2. Also, there is a potential to remove more states as we have seen that a minimal realization might require an even smaller state-space. However, it remains an open question how this information can be used to obtain reduced-order systems. In what follows, we propose a method enabling to identify simultaneously the states that are unreachable and unobservable. For this, we assume that

$$\text{rank}\left(\left[\mathbf{W}^\top\mathbf{A}_1\mathbf{V},\ \dots\ ,\mathbf{W}^\top\mathbf{A}_l\mathbf{V}\right]\right) = \text{rank}\left(\begin{bmatrix}\mathbf{W}^\top\mathbf{A}_1\mathbf{V}\\ \vdots \\ \mathbf{W}^\top\mathbf{A}_l\mathbf{V}\end{bmatrix}\right) = r, \tag{17}$$

where $\mathbf{V}$ and $\mathbf{W}$ are the matrices defined in Equation (15a,b) encoding, respectively, the reachability and the observability subspaces, that is, $\text{range}(\mathbf{V}) = \mathcal{V}_R$ and $\text{range}(\mathbf{W}) = \mathcal{W}_O$ and $\mathbf{A}_i, i \in \{1,\ \dots\ ,l\}$, are defined in (2). Using the matrices appearing in (17), we will be able to extract simultaneously the subspaces that are unobservable and unreachable from the original system To this aim, we consider the compact SVDs

$$\left[\mathbf{W}^\top\mathbf{A}_1\mathbf{V},\ \dots\ ,\mathbf{W}^\top\mathbf{A}_l\mathbf{V}\right] = \mathbf{W}_1\Sigma_l\widetilde{\mathbf{V}}^\top \quad \text{and} \quad \begin{bmatrix}\mathbf{W}^\top\mathbf{A}_1\mathbf{V}\\ \vdots \\ \mathbf{W}^\top\mathbf{A}_l\mathbf{V}\end{bmatrix} = \widetilde{\mathbf{W}}\Sigma_r\mathbf{V}_1^\top. \tag{18}$$

Let $\mathbf{W}_p := \mathbf{W}\mathbf{W}_1$ and $\mathbf{V}_p := \mathbf{V}\mathbf{V}_1$ be two truncation matrices and let us consider the lower-order realization $\widehat{\mathcal{C}}_p(s,\mathbf{p})\widehat{\mathcal{K}}_p(s,\mathbf{p})^{-1}\widehat{\mathcal{B}}_p(s,\mathbf{p})$ constructed by Petrov-Galerkin projection as follows:

$$\widehat{\mathcal{B}}_p(s,\mathbf{p}) = \mathbf{W}_p^\top\mathcal{B}(s,\mathbf{p}), \quad \widehat{\mathcal{C}}_p(s,\mathbf{p}) = \mathcal{C}(s,\mathbf{p})\mathbf{V}_p, \quad \widehat{\mathcal{K}}_p(s,\mathbf{p}) = \mathbf{W}_p^\top\mathcal{K}(s,\mathbf{p})\mathbf{V}_p. \tag{19}$$

Then, the following result holds.

Theorem 3. *The lower-order system* $\widehat{C}_p(s,\mathbf{p})\widehat{\mathcal{K}}_p(s,\mathbf{p})^{-1}\widehat{\mathcal{B}}_p(s,\mathbf{p})$ *of order* r, *obtained as given in Equation* (19), *realizes the original transfer function, that is,*

$$\widehat{C}_p(s,\mathbf{p})\widehat{\mathcal{K}}_p(s,\mathbf{p})^{-1}\widehat{\mathcal{B}}_p(s,\mathbf{p}) = C(s,\mathbf{p})\mathcal{K}(s,\mathbf{p})^{-1}\mathcal{B}(s,\mathbf{p})$$

for every $s \in \mathbb{C}$ *and* $\mathbf{p} \in \Omega^d$.

Proof. Recall that $\mathbf{V}_p = \mathbf{V}\mathbf{V}_1$ and $\mathbf{W}_p = \mathbf{W}\mathbf{W}_1$. Hence, by construction, range $(\mathbf{V}_p) \subseteq$ range $(\mathbf{V}) = \mathcal{V}_R$ and range $(\mathbf{W}_p) \subseteq$ range $(\mathbf{W}) = \mathcal{W}_O$. Hence, there exist $\mathbf{V}_a$ and $\mathbf{W}_a$, $\mathbf{V}_a \perp \mathbf{V}_p$ and $\mathbf{W}_a \perp \mathbf{W}_p$ such that range$\left(\begin{bmatrix}\mathbf{V}_p & \mathbf{V}_a\end{bmatrix}\right) = \mathcal{V}_R$ and range $\left(\begin{bmatrix}\mathbf{W}_p & \mathbf{W}_a\end{bmatrix}\right) = \mathcal{W}_O$. As a consequence, from the compact SVDs in (18),

$$\mathbf{W}^\top\mathbf{A}_k\mathbf{V}_a = 0, \quad \mathbf{W}_a^\top\mathbf{A}_k\mathbf{V} = 0, \quad \text{and} \quad \mathbf{W}_a^\top\mathbf{A}_k\mathbf{V}_a = 0, \text{ for } k \in \{1, \dots, l\},$$

and hence,

$$\mathbf{W}_p^\top\mathcal{K}(s,\mathbf{p})\mathbf{V}_a = 0, \quad \mathbf{W}_a^\top\mathcal{K}(s,\mathbf{p})\mathbf{V}_p = 0, \quad \text{and} \quad \mathbf{W}_a^\top\mathcal{K}(s,\mathbf{p})\mathbf{V}_a = 0.$$

Moreover, notice that

$$\mathcal{K}(s,\mathbf{p})^{-1}\mathcal{B}(s,\mathbf{p}) = \begin{bmatrix}\mathbf{V}_p & \mathbf{V}_a\end{bmatrix}\begin{bmatrix}\widehat{\mathcal{K}}_p(s,\mathbf{p})^{-1}\widehat{\mathcal{B}}_p(s,\mathbf{p}) \\ \star\end{bmatrix} \quad \text{and}$$

$$C(s,\mathbf{p})\mathcal{K}(s,\mathbf{p})^{-1} = \begin{bmatrix}\widehat{C}_p(s,\mathbf{p})\widehat{\mathcal{K}}_p(s,\mathbf{p})^{-1} & \star\end{bmatrix}\begin{bmatrix}\mathbf{W}_p^\top \\ \mathbf{W}_a^\top\end{bmatrix}.$$

Finally, we write

$$\begin{aligned}
C(s,\mathbf{p})\mathcal{K}(s,\mathbf{p})^{-1}\mathcal{B}(s,\mathbf{p}) &= C(s,\mathbf{p})\mathcal{K}(s,\mathbf{p})^{-1}\mathcal{K}(s,\mathbf{p})\mathcal{K}(s,\mathbf{p})^{-1}\mathcal{B}(s,\mathbf{p}) \\
&= \begin{bmatrix}\widehat{C}(s,\mathbf{p})\widehat{\mathcal{K}}(s,\mathbf{p})^{-1} & \star\end{bmatrix}\begin{bmatrix}\mathbf{W}_p^\top \\ \mathbf{W}_a^\top\end{bmatrix}\mathcal{K}(s,\mathbf{p})\begin{bmatrix}\mathbf{V}_p & \mathbf{V}_a\end{bmatrix}\begin{bmatrix}\widehat{\mathcal{K}}(s,\mathbf{p})^{-1}\widehat{\mathcal{B}}(s,\mathbf{p}) \\ \star\end{bmatrix} \\
&= \begin{bmatrix}\widehat{C}(s,\mathbf{p})\widehat{\mathcal{K}}(s,\mathbf{p})^{-1} & \star\end{bmatrix}\begin{bmatrix}\mathbf{W}_p^\top\mathcal{K}(s,\mathbf{p})\mathbf{V}_p & 0 \\ 0 & 0\end{bmatrix}\begin{bmatrix}\widehat{\mathcal{K}}(s,\mathbf{p})^{-1}\widehat{\mathcal{B}}(s,\mathbf{p}) \\ \star\end{bmatrix} \\
&= \widehat{C}(s,\mathbf{p})\widehat{\mathcal{K}}(s,\mathbf{p})^{-1}\widehat{\mathcal{K}}(s,\mathbf{p})\widehat{\mathcal{K}}(s,\mathbf{p})^{-1}\widehat{\mathcal{B}}(s,\mathbf{p}) = \widehat{C}(s,\mathbf{p})\widehat{\mathcal{K}}(s,\mathbf{p})^{-1}\widehat{\mathcal{B}}(s,\mathbf{p}),
\end{aligned}$$

which concludes the proof. ∎

Theorem 3 shows that if we construct the lower-order system as shown in Equation (19), it also realizes the original system. As a consequence, the rank condition Equation (17) gives us the order r of the lower-order realization constructed by Petrov Galerkin projection, which realizes the original system. Hence, the matrices

$$\begin{bmatrix}\mathbf{W}^\top\mathbf{A}_1\mathbf{V}, \dots, \mathbf{W}^\top\mathbf{A}_l\mathbf{V}\end{bmatrix} \quad \text{and} \quad \begin{bmatrix}\mathbf{W}^\top\mathbf{A}_1\mathbf{V} \\ \vdots \\ \mathbf{W}^\top\mathbf{A}_l\mathbf{V}\end{bmatrix} \tag{20}$$

encode the complexity of the original system. Moreover, by means of the compact SVDs of these matrices, we are able to find the projection matrices $\mathbf{V}_p = \mathbf{V}\mathbf{V}_1$ and $\mathbf{W}_p = \mathbf{W}\mathbf{W}_1$, leading to a lower-order system having the same transfer function as the original one. Hence, the states that are removed from the dynamics of the original systems can be seen as unreachable or unobservable ones. On the other hand, the singular values in Σ_r and Σ_l give some important information

about the simultaneous degree of reachability and observability of the states. Indeed, states that are related to small singular values can be interpreted to have a weak simultaneous degree of reachability and observability, while the states related to large singular values are strongly simultaneously reachable and observable. Therefore, removing also the subspaces associated with small singular values leads to reduced-order systems.

4 | MODEL ORDER REDUCTION ALGORITHM

Based on the arguments given in the previous section, we propose Algorithm 1 for constructing reduced-order systems for structured systems (12). The procedure consists in selecting interpolation points $(s_i, \mathbf{p}_i)$ and constructs the matrices $\mathbf{V}$ and $\mathbf{W}$ as in (6a,b) (Steps 2 and 3). If we have enough interpolation points, the subspaces range ($\mathbf{V}$) and range ($\mathbf{W}$) mimic the reachable subspace $\mathcal{V}_R$ and the observable subspace $\mathcal{W}_O$, respectively. Then, in Step 4, we compute the SVDs of the matrices in (22). As previously discussed, the numerical rank of those matrices provides an estimate of where to truncate to obtain a reduced-order system. Hence, in Step 5, the projection matrices $\mathbf{V}_p$ and $\mathbf{W}_p$ are constructed according to Theorem 3. Finally, in Step 6, the reduced-order system is determined by Petrov-Galerkin projection.

Remark 2. So far in the paper, we have refrained from discussing the idea of tangential interpolation. In the case of multi-input multi-output (MIMO) systems, one can employ the idea of tangential interpolation which has been proven to be very useful in the MIMO case.[31] For this, along with considering interpolation points $\{\sigma_i, \mathbf{p}_i\}$ and $\{\mu_j, \mathbf{q}_j\}$, we also consider tangential directions $\mathbf{b}_i$ and $\mathbf{c}_j$ of appropriate sizes. For details, we refer to for example, Reference 17. Hence, with the tangential directions, the analogues of matrices $\mathbf{V}$ and $\mathbf{W}$ in (16a,b) are

$$\mathbf{V} = \begin{bmatrix} \mathcal{K}(\sigma_1, \mathbf{p}_1)^{-1}\mathcal{B}(\sigma_1, \mathbf{p}_1)\mathbf{b}_1, \ \dots\ , \mathcal{K}(\sigma_N, \mathbf{p}_N)^{-1}\mathcal{B}(\sigma_N, \mathbf{p}_N)\mathbf{b}_N \end{bmatrix},$$
$$\mathbf{W} = \begin{bmatrix} \mathcal{K}(\sigma_1, \mathbf{p}_1)^{-\top}\mathcal{C}(\sigma_1, \mathbf{p}_1)^{\top}\mathbf{c}_1^{\top}, \ \dots\ , \mathcal{K}(\sigma_N, \mathbf{p}_N)^{-\top}\mathcal{C}(\sigma_N, \mathbf{p}_N)^{\top}\mathbf{c}_N^{\top} \end{bmatrix}.$$

Hence, these matrices can be used in Step 3 of Algorithm 1.

Remark 3. One of the additional advantages of the proposed algorithm is that it inherently allows to construct frequency-limited reachable and observable subspaces by choosing the interpolation points in a given frequency range. Hence, it yields a reduced-order system that is good in the considered frequency range.

Remark 4. The proposed framework is also suitable for non-dynamical linear parametric systems, that is, systems of the form

$$\mathbf{A}(\mathbf{p})\mathbf{x}(\mathbf{p}) = \mathbf{B}(\mathbf{p}),$$
$$\mathbf{y}(\mathbf{p}) = \mathbf{C}(\mathbf{p})\mathbf{x}(\mathbf{p}).$$

In this case, the solution $\mathbf{y}(\mathbf{p})$ can be obtained as

$$\mathbf{y}(\mathbf{p}) = \mathbf{C}(\mathbf{p})\mathbf{A}(\mathbf{p})^{-1}\mathbf{B}(\mathbf{p}),$$

and the reachability and observability subspaces, namely $\mathcal{V}_R$ and $\mathcal{W}_O$, are the smallest subspaces such that range $\left(\mathbf{A}(\mathbf{p})^{-1}\mathbf{B}(\mathbf{p})\right) \subset \mathcal{V}_R$ and range $\left(\mathbf{A}(\mathbf{p})^{-\top}\mathbf{C}(\mathbf{p})^{\top}\right) \subset \mathcal{W}_O$ for all $\mathbf{p} \in \Omega^d$. In this case, we determine dominant subsystems with respect to parameters using Algorithm 1.

Remark 5. In several applications, it is highly desirable to determine reduced-order systems via one-sided projection in order to potentially preserve some important properties of the systems such as stability or passivity. In this case, in Step 3 of Algorithm 1, we set $\mathbf{W} = \mathbf{V}$, and in Step 5 of Algorithm 1, we again set $\mathbf{W}_p = \mathbf{V}_p$.

Remark 6. It is worth noticing that the matrix $\mathbf{V}$ in (16a) satisfies the generalized Sylvester equation

$$\sum_{i=1}^{l} \mathbf{A}_i \mathbf{V} \mathbf{\Pi}_i = \sum_{i=1}^{q} \mathbf{B}_i \begin{bmatrix} 1, \ \dots\ , 1 \end{bmatrix} \mathbf{\Gamma}_i, \tag{21}$$

where $\mathbf{\Pi}_i = \operatorname{diag}\big(\kappa_i(\sigma_1, \mathbf{p}_1), \ \dots \ , \kappa_i(\sigma_N, \mathbf{p}_N)\big)$ and $\mathbf{\Gamma}_i = \operatorname{diag}\big(\beta_i(\sigma_1, \mathbf{p}_1), \ \dots \ , \beta_i(\sigma_N, \mathbf{p}_N)\big)$. Hence, one possible way to obtain $\mathbf{V}$ in Step 3 of Algorithm 1, is by solving the generalized Sylvester Equation (21). In a large-scale setting, one can use low rank methods such as References 32–34 to solve those linear matrix equations. A detailed discussion on numerical methods of the matrix Equation (21) is not within the scope of this paper.

Remark 7. In the above remark, we have discussed that the matrix $\mathbf{V}$ can be constructed efficiently by solving a corresponding Sylvester equation. However, one should also notice that the columns of the matrix $\mathbf{V}$ solve a linear system with different interpolation points; see (15a). Therefore, these columns can also be constructed independently, thus in an embarrassingly parallelizable fashion.

Algorithm 1. Construction of ROMs via **D**ominant **R**eachable and **O**bservable subspace-based **P**rojection (**DROP**)

1: **Input:** The transfer function as in (4), and tolerance `tol`.
2: Choose interpolation points for frequency and parameters to construct $\mathbf{V}$ and $\mathbf{W}$.
3: Compute $\mathbf{V}$ and $\mathbf{W}$ using the interpolation points as in (6).
4: Determine SVDs

$$\left[\mathbf{W}^\top \mathbf{A}_1 \mathbf{V}, \dots, \mathbf{W}^\top \mathbf{A}_l \mathbf{V}\right] = \mathbf{W}_1 \Sigma_l \widetilde{\mathbf{V}}^\top \quad \text{and} \quad \begin{bmatrix} \mathbf{W}^\top \mathbf{A}_1 \mathbf{V} \\ \vdots \\ \mathbf{W}^\top \mathbf{A}_l \mathbf{V} \end{bmatrix} = \widetilde{\mathbf{W}} \Sigma_r \mathbf{V}_1^\top \tag{22}$$

with $\Sigma_l = \operatorname{diag}\left(\sigma_1^l, \dots, \sigma_N^l\right)$ and $\Sigma_r = \operatorname{diag}\left(\sigma_1^r, \dots, \sigma_N^r\right)$.
5: Compute order of reduced system r as

$$r = \max\{r_l, r_r\},$$

where r_l and r_r are, respectively, the number of singular values σ_k^l that are larger than `tol` and the number of singular values σ_k^r that are larger than `tol`.
6: Compute projection matrices:$\mathbf{V}_p = \mathbf{V}\mathbf{V}_1(:, 1\!:\!r)$ and $\mathbf{W}_p = \mathbf{W}\mathbf{W}_1(:, 1\!:\!r)$.
7: Compute reduced matrices:

$$\widehat{\mathcal{K}}(s, \mathbf{p}) = \mathbf{W}_p^\top \mathcal{K}_s(s) \mathbf{V}_p, \quad \widehat{\mathcal{B}}(s, \mathbf{p}) = \mathbf{W}_p^\top \mathcal{B}(s, \mathbf{p}), \text{ and } \quad \widehat{\mathcal{C}}(s, \mathbf{p}) = \mathcal{C}(s, \mathbf{p}) \mathbf{V}_p.$$

8: **Output:** The reduced-order matrices: $\widehat{\mathcal{K}}(s, \mathbf{p})$, $\widehat{\mathcal{B}}(s, \mathbf{p})$, and $\widehat{\mathcal{C}}(s, \mathbf{p})$.

5 | NUMERICAL RESULTS

In this section, we illustrate the efficiency of the proposed methods via several numerical examples, arising in various applications. For the non-parametric case, we also compare with the existing methods proposed in References 1,11, and for the parametric case with the adaptive interpolation method proposed in Reference 35. We have performed all the simulations on a board with 4 Intel® Xeon® E7-8837 CPUs with a 2.67-GHz clock speed using MATLAB 8.0.0.783 (R2016b). Furthermore, we generate random numbers, whenever necessary, using `rng(0, 'twister')`. In the case of a MIMO system, we determine the projection matrices by employing the idea of tangential interpolation, and we choose the tangential directions randomly.

5.1 | A demo example

At first, we discuss an artificial example to illustrate the proposed method. Let us consider a system of order $n = 3$ as follows:

$$\begin{bmatrix} 1 & 0 & 0 \\ 0 & 1 & 0 \\ 0 & 0 & 1 \end{bmatrix} \dot{\mathbf{x}}(t) = \begin{bmatrix} -2 & 0 & 0 \\ 0 & -1 & 0 \\ 0 & 0 & -2 \end{bmatrix} \mathbf{x}(t) + \mathbf{p} \begin{bmatrix} 0 & 1 & 0 \\ -1 & 0 & 0 \\ 1 & 0 & 0 \end{bmatrix} \mathbf{x}(t) + \begin{bmatrix} 1 \\ 0 \\ 1 \end{bmatrix} \mathbf{u}(t),$$
$$\mathbf{y}(t) = \begin{bmatrix} 1 & 1 & 0 \end{bmatrix} \mathbf{x}(t). \tag{23}$$

The example is constructed in such a way that the parameter $\mathbf{p}$ changes the imaginary parts of two eigenvalues of the system. Hence, with a change of the parameter, we expect a change in the peak of the transfer function.

Next, we aim at constructing a reduced realization of the system Equation (23) by employing Algorithm 1. For this, we take 10 points for the frequency $s \in [10^{-4}, 10]$ and for the parameter $\mathbf{p} \in [-10, 10]$. We take the frequency points in the given range in logarithmic scale, whereas the parameters are chosen randomly in the considered parameter range. In Figure 1, we plot the decay of the singular values as computed in Step 4 of Algorithm 1. It can be observed that the first two singular values are non neglectable, and the others are at the level of machine precision. This suggests that a reachable and observable system, representing the input/output behavior of the system (23) has the order exactly $r = 2$. We compare the transfer functions of the original and reduced-order systems for 20 linearly spaced parameter values in $[-10, 10]$, which are plotted in Figure 2. The figure shows that the error between the original and reduced-order system is of the level of machine precision.

The order 2 of a minimal realization can also be easily verified by analyzing the system (23). Notice that $x_3(t)$ does not influence the dynamics of $x_1(t)$ and $x_2(t)$, where $x_i(t)$ denotes the ith component of the vector $x(t)$, and $x_3(t)$ is not being observed due to the output matrix $\mathbf{C} = [1, 1, 0]$. Hence, $x_3(t)$ can be eliminated as far as the input-output dynamics are concerned. Therefore, the system (23) can exactly be reduced to order 2.

5.2 | Time-delay system

Next, we consider the time-delay model[13] of order n,

$$\begin{aligned} \mathbf{E}\dot{\mathbf{x}}(t) &= \mathbf{A}\mathbf{x}(t) + \mathbf{A}_\tau \mathbf{x}(t-\tau) + \mathbf{B}\mathbf{u}(t), \\ \mathbf{y}(t) &= \mathbf{C}\mathbf{x}(t), \end{aligned} \tag{24}$$

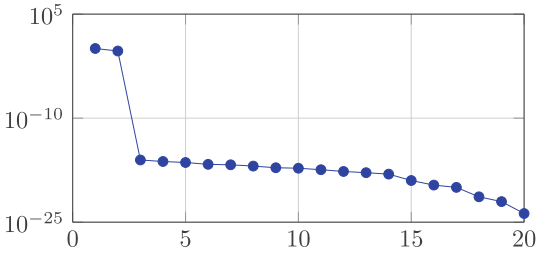

FIGURE 1 Demo example: Decay of the singular values.

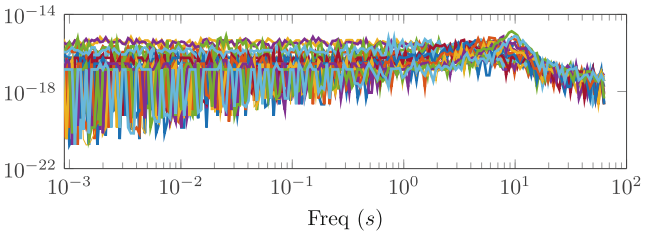

FIGURE 2 Demo example: The figure shows the Bode plot of the error between the original and reduced-order systems for different parameter values. Each color represents the error for a different parameter.

where $\mathbf{E} = \mu\mathbf{I}_n + \mathbf{T}$, $\mathbf{A} = \frac{1}{\tau}\left(\frac{1}{\zeta} + 1\right)(\mathbf{T} - \mu\mathbf{I}_n)$, and $\mathbf{A}_\tau = \frac{1}{\tau}\left(\frac{1}{\zeta} - 1\right)(\mathbf{T} - \mu\mathbf{I}_n)$ in which the matrix $\mathbf{T}$ is such that it is ones on the sub- and super-diagonal along with the $(1, 1)$ and (n, n) elements. The input matrix $\mathbf{B}$ is zero everywhere except for the first and second entries, that is, $\mathbf{B}(1) = \mathbf{B}(2) = 1$, and the output matrix is $\mathbf{C} = \mathbf{B}^\top$. Furthermore, we choose $\mu = 5$, $\zeta = 0.01$, $\tau = 1$, and the order $n = 500$.

Next, we aim at constructing reduced-order systems using balanced truncation as proposed in Reference 11 and using Algorithm 1. In order to apply Algorithm 1, we take 1000 logarithmically distributed frequency points in the range $\left[10^{-2}, 10^{4}\right]$. Furthermore, to apply balanced truncation, we need to determine the system Gramians, which are given in integral forms. To compute approximations of the Gramians, we make of use of the `quadv` command in MATLAB with `tol` $= 10^{-10}$ to integrate in the given frequency range.

First, we plot the singular values, obtained from balanced truncation and Algorithm 1 in Figure 3, which indicates a faster decay of singular values obtained from Algorithm 1. We now determine reduced-order systems of order $r = 12$ using both methods. We compare the Bode plots of the original and reduced-order systems in Figure 4. The figure shows that both methods capture the dynamics very well; however, our method clearly yields a better reduced-order system at least by two orders of magnitudes at most frequencies.

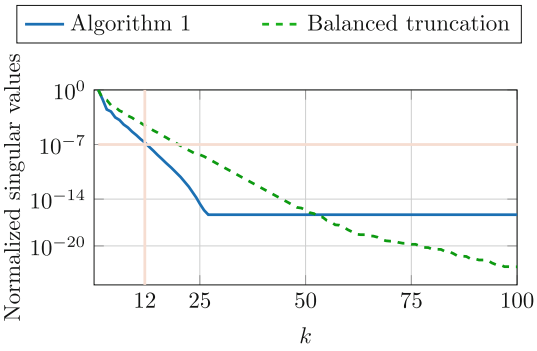

FIGURE 3 Time-delay example: Relative decay of the singular values using Algorithm 1 and structured balanced truncation.

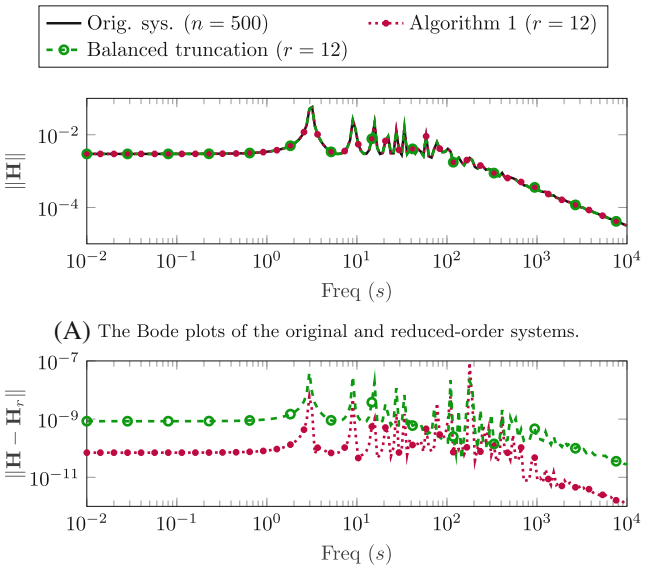

(A) The Bode plots of the original and reduced-order systems.

(B) The Bode plots of the errors of the reduced-order systems.

FIGURE 4 Time-delay example: The figure presents a comparison of the Bode plots of the original and reduced-order systems. (A) The Bode plots of the original and reduced-order systems. (B) The Bode plots of the errors of the reduced-order systems.

5.3 | Heat equation with fading memory

We consider the heat equation with fading memory presented in Reference 11. Its dynamics are governed by the following integro-PDE:

$$\begin{aligned} v_t(t,x) &= \Delta v(t,x) - \int_0^t \gamma(t-s)\Delta v(s,x)ds + \chi_\omega \mathbf{u}(t) \quad \text{in } (0,\infty)\times\Omega, \\ v(t,x) &= 0 \quad \text{in } (0,\infty)\times\Gamma, \qquad v(0,x) = 0 \quad \text{in } \Omega, \\ v_{obs}(\cdot) &= \int_\Omega v(\cdot,x)dx, \end{aligned} \tag{25}$$

where $\gamma = 1.05$, $\Omega = (0,1)\times(0,1)$, Γ denotes the boundary of Ω and χ_ω is the characteristic function of the control set $\omega = [0.15, 0.25]\times[0.2, 0.3] \subset \Omega$, i.e.,

$$\chi_\omega(x) := \begin{cases} 1, & \text{if } x \in \omega, \\ 0, & \text{otherwise.} \end{cases}$$

As discussed in Reference 11, after spatial discretization by a finite difference method, we obtain a Volterra integro-differential system whose transfer function is given by

$$\mathbf{H}(s) = \mathbf{C}\left(s\mathbf{I} - \mathbf{A} + \tfrac{1}{s+\gamma}\mathbf{A}\right)^{-1}\mathbf{B}. \tag{26}$$

We consider 128 grid points in each direction, leading to a system of order $n = 16{,}384$. In Figure 5, we first plot the relative singular values obtained using Algorithm 1 and balanced truncation from Reference 11. The figure shows that a very low-order model is possible to obtain having very high accuracy. We determine reduced-order systems of order $r = 3$ using both methods. We compare both reduced-order systems in Figure 6A, which shows that the reduced-order systems are comparable. Moreover, in Figure 6B, we show the $\mathcal{H}_2$-norm of the error systems with respect to the order of the reduced-order system. This also indicates that both methods produce reduced-order systems of very similar quality.

5.4 | Fractional Maxwell equations

Next, we consider the example mentioned in the introduction arising in computational electromagnetics, see Reference 1. As described in the introduction, the transfer function of this example has a fractional integrator of the form:

$$\mathbf{H}(s) = s\mathbf{B}^\top\left(s^2\mathbf{I} - \frac{1}{\sqrt{s}}\mathbf{D} + \mathbf{A}\right)^{-1}\mathbf{B}, \tag{27}$$

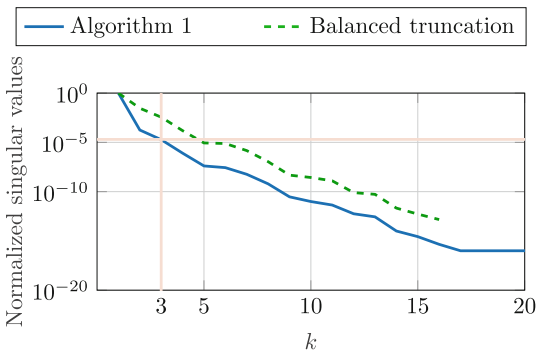

FIGURE 5 Heat equation with fading memory: Relative decay of the singular values using Algorithm 1 and structured balanced truncation.

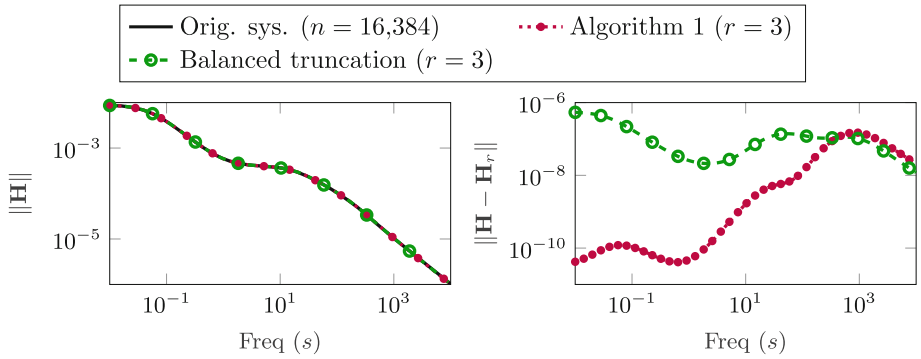

(A) The Bode plots of the original, reduced-order systems, and the error system.

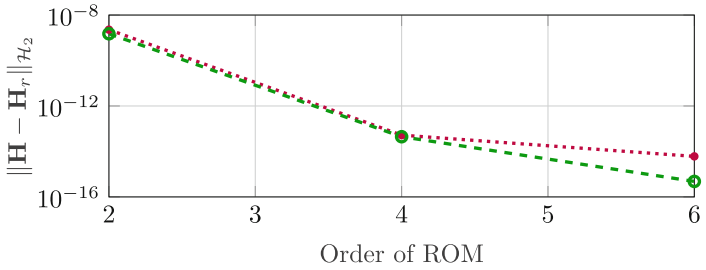

(B) The relative errors of the reduced-order systems.

FIGURE 6 Heat equation with fading memory: The figure presents a comparison of the Bode plots of the original and reduced-order systems for order $r = 3$, and $\mathcal{H}_2$-norm of the error with respect to the order of the reduced-order systems. (A) The Bode plots of the original, reduced-order systems, and the error system. (B) The relative errors of the reduced-order systems.

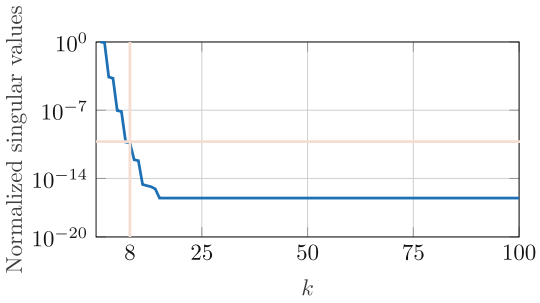

FIGURE 7 Fractional Maxwell equations: Relative decay of the singular values using Algorithm 1.

where $n = 29{,}295$ is the order, $\mathbf{I}, \mathbf{A}$ and $\mathbf{D}$ are $n \times n$ matrices, and $\mathbf{B}$ is an $n \times 1$ matrix. In this example, the interesting frequency range is $\mathcal{F} := [4 \cdot 10^9, 8 \cdot 10^9]$Hz. We aim at employing Algorithm 1 and balanced truncation. Although the proposed balanced truncation method from Reference 11 is not designed for limited frequency range, one can integrate over $\mathcal{F}$ instead of $[0, \infty]$ to determine the Gramians. However, we observe that for this example, the methodology proposed in Reference 11 to obtain an approximation in low-rank factor form does not converge. As discussed in Reference 11, the development of low-rank solvers for Gramians of structure systems needs some future research which is highly relevant to this. Moreover, since the example is a large-scale one, it is not possible to apply the simple `quadv` function to obtain approximations of Gramians as we did in the delay example.

We instead compare our methodology to the method proposed in Reference 1, where a reduced-order system is obtained using moment-matching based on a single expansion point. In order to employ Algorithm 1, we take 50 points in logarithmic scale in the frequency range of interest. First, we plot the relative decay of the singular values in Figure 7. Ideally, we would like to determine a reduced-order system of order $r = 38$, which is reported in Reference 1. However, our decay of singular values indicates that the order more than 10 would not improve the quality of the reduced-order system as the singular values go to the level of machine precision. Therefore, we determine the reduced-order system of

order $r = 8$ via our method and compare with the reduced-order system of order $r = 38$ as constructed in Reference 1. In Figure 8, we compare both reduced-order systems. The figure suggests that our reduced-order system outperforms the one reported in Reference 1. Importantly, notice that this is achieved even though our reduced-order system has an order more than four times smaller than the one from Reference 1. On the other hand, we have used 50 sparse factorizations in contrast to only one as used in Reference 1. This shows a bit of the trade-off of the proposed method compared to earlier attempts to generalize moment-matching methods to structured linear systems.

5.5 | Parametric anemometer

An anemometer, also known as a thermal mass flow meter, has sensors, namely heater and temperature after and before the heater in the direction of the flow as shown in Figure 9. Due to the circulation of the flow, a temperature difference occurs between the sensors. Measuring the temperature difference allows to estimate the fluid flow, for more details see Reference 36.

The dynamics of the anemometer is governed by the convection-diffusion PDE

$$\rho c \frac{\partial T}{\partial t} = \nabla \cdot (\kappa \nabla T) - \rho c v \nabla T + \dot{q}, \tag{28}$$

where ρ represents the mass density; c, κ, v are the specific heat, thermal conductivity, and fluid velocity, respectively. Moreover, $\dot{q}$ denotes the heat flow into the system caused by the heater. We set $\rho = 1$ and consider all other fluid properties as parameters. A discretization of the PDE leads to a parametric system whose transfer function is given by

$$\mathbf{H}(s, \mathbf{p}) = \mathbf{C}(s(\mathbf{E}_0 + p_1\mathbf{E}_1) - (\mathbf{A}_0 + p_2\mathbf{A}_1 + p_3\mathbf{A}_2))^{-1}\mathbf{B},$$

where $\mathbf{p} \in \mathbb{R}^3$ and p_i denotes the ith component of the vector $\mathbf{p}$, which is given in terms of the fluid properties as follows:

$$\mathbf{p}^\top = \begin{bmatrix} p_1 & p_2 & p_3 \end{bmatrix}^\top = \begin{bmatrix} c & \kappa & cv \end{bmatrix}^\top.$$

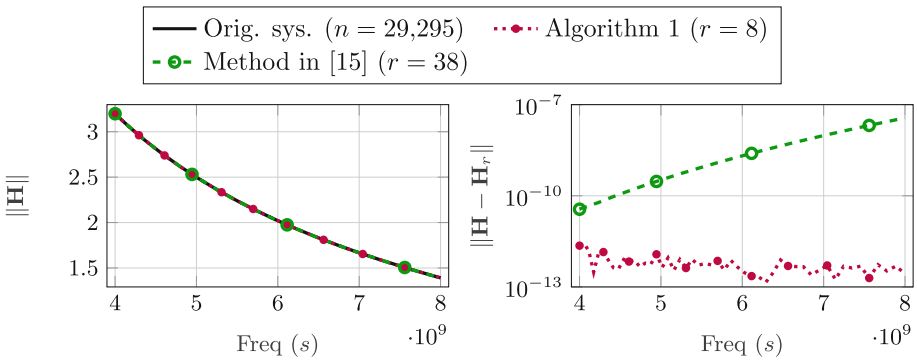

FIGURE 8 Fractional Maxwell equations: The Bode plots of the original, reduced-order systems, and the error system.

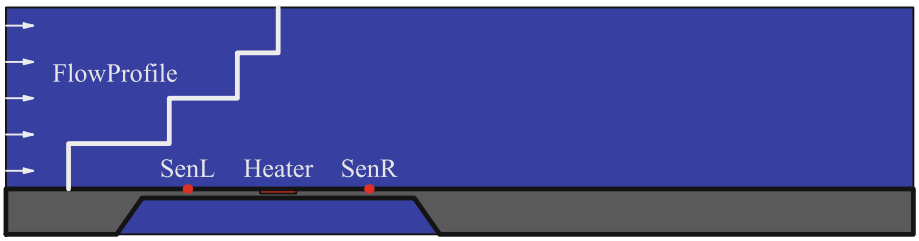

FIGURE 9 Schematic diagram of a two-dimensional anemometer, compare Reference 37.

The output matrix $\mathbf{C}$ is chosen such that it yields the output as the difference between the two sensors. For more details, we refer to Reference 38 and for the model, to Reference 37. A finite-element discretization yields a parametric model of order $n = 29{,}008$, and the model essentially has three parameters. It is worth mentioning that the stationary problem, that is, when the left-hand side of Equation (28) is zero, would lead to a transfer function that does not depend on s and p_1, but only on p_2 and p_2. In this case, we are in the setup of non-dynamical linear parametric systems, and Algorithm 1 can still be used to construct a surrogate model, as described in Remark 4.

In order to apply the proposed method, we take 300 points for frequency s in logarithmic scale and 300 random points for the parameters. For this example, the most relevant frequency range is $[10^1, 10^5]$, and the parameters are chosen as follows: $c \in [0, 1]$, $\kappa \in [1, 2]$, and $\nu \in [0.1, 2]$. First, in Figure 10, we plot the singular values, obtained by employing Algorithm 1, which exhibits a rapid decay. We now determine reduced-order systems of order $r = 78$, meaning that we consider the singular vectors corresponding to the relative singular values up-to 10^{-6}. We compare the Bode plots of the original and reduced-order systems in Figure 11 for two different parameter values, which clearly match for both parameters all frequencies.

Moreover, in Figure 12, we plot the Bode diagram of the error systems, the difference of the original and reduced-order systems, for different parameter configurations. The obtained reduced-order system captures the dynamics of the original

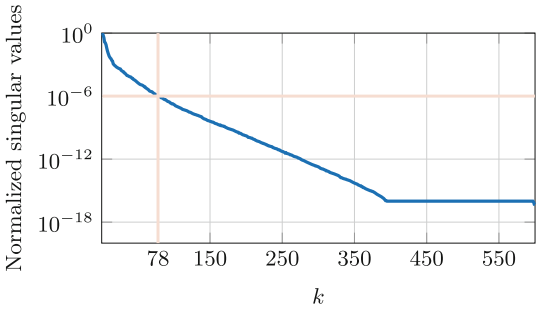

FIGURE 10 Anemometer example: Relative decay of the singular values using Algorithm 1.

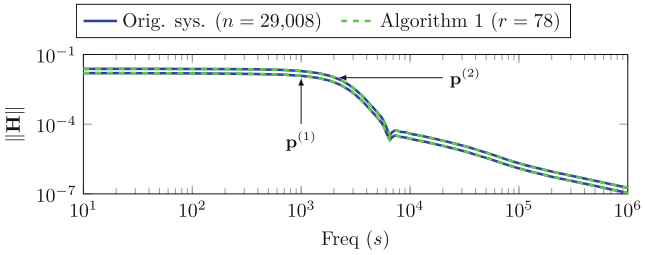

FIGURE 11 Anemometer example: The Bode plots of the original and reduced-order systems for parameter values $\mathbf{p}^{(1)} = (0, 1, 0.1)$ and $\mathbf{p}^{(2)} = (0.67, 1.67, 1.37)$.

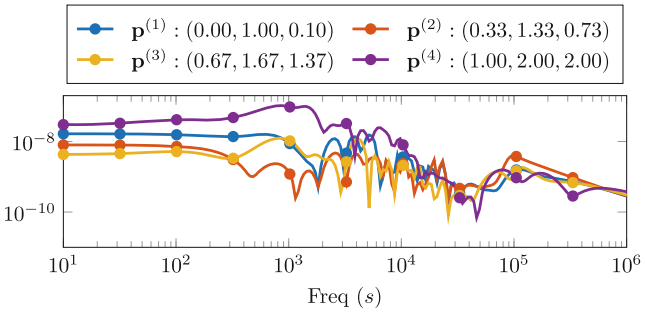

FIGURE 12 Anemometer example: The Bode plots of the absolute error between the original and the reduced-order systems for four different parameter values.

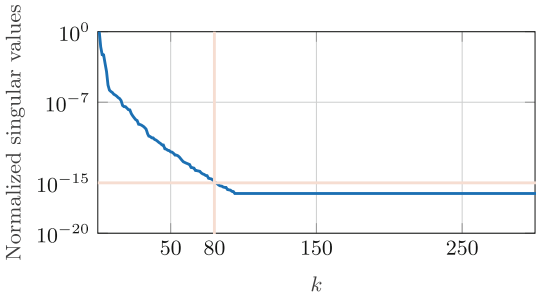

FIGURE 13 Gyro example: Relative decay of the singular values obtained using Algorithm 1.

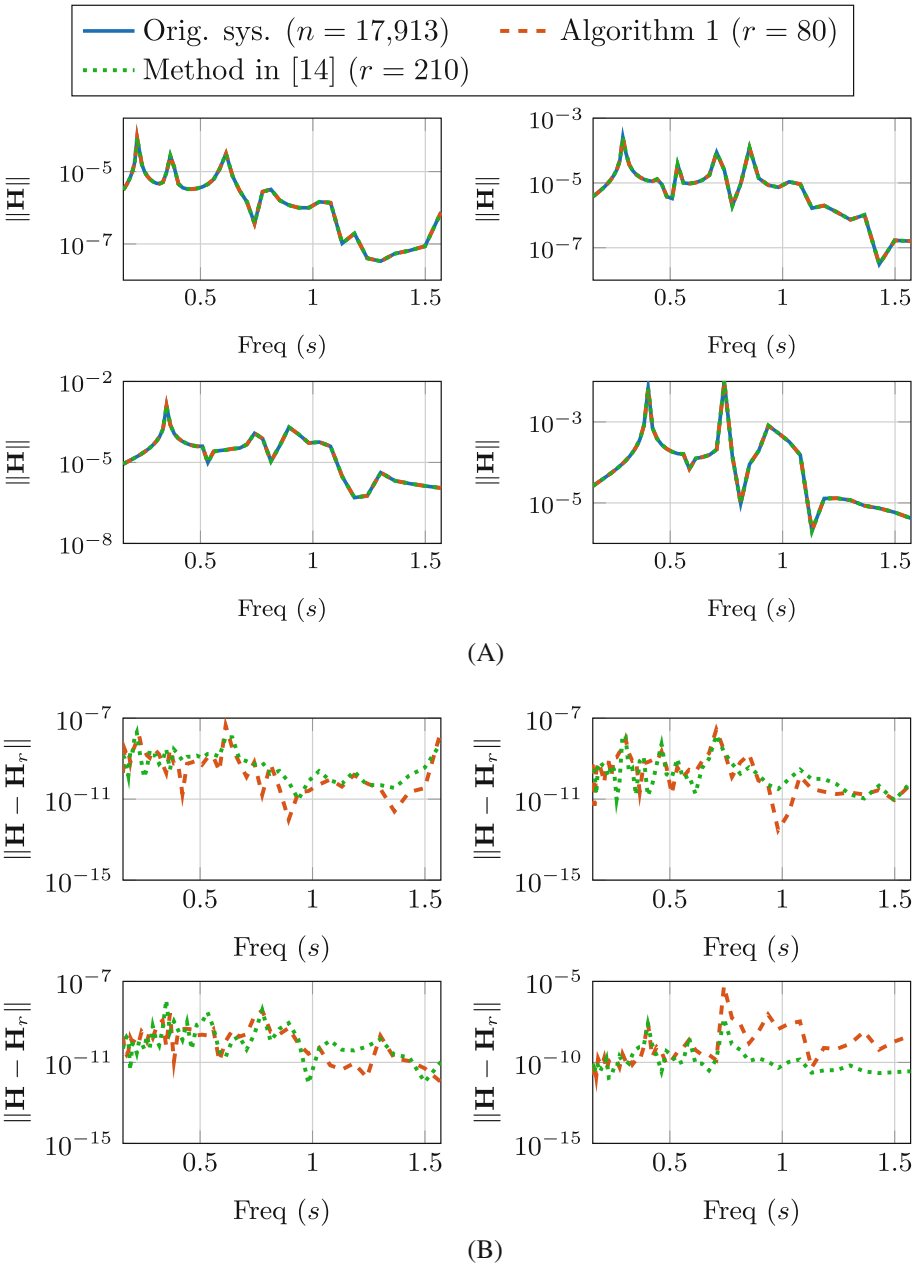

FIGURE 14 Gyro example: A comparison of the original and reduced-order systems for different parameters values. (A) The Bode plots of the original and reduced-order systems for parameter values $\mathbf{p}(1)$: $(1.00; 10^{-7})$ at the top-left, $\mathbf{p}(2)$: $(1.33; 4.64 \cdot 10^{-7})$ at the top-right, $\mathbf{p}(3)$: $(1.67; 2.15 \cdot 10^{-6})$ at the bottom-left and $\mathbf{p}(4)$: $(2.00; 10^{-5})$ at the top-right. (B) The Bode plots of the absolute error between the original and reduced-order systems for the above considered parameter values.

systems very well. From the figures, it can be seen that the error is below $2 \cdot 10^{-7}$ for all frequencies and four considered parameter configurations.

5.6 | Parametric butterfly gyroscope

As the last example, we consider a parametric butterfly gyroscope example. The butterfly is a vibrating micro-mechanical gyro, which measures angular rates in up to three axes. It is used in inertial navigation applications. The model has mainly two parameters of interest: the rotation velocity θ around the x-axis and the width of bearing d. The system and its model reduction problem have been extensively studied in Reference 39. A finite element discretization leads to a parametric model for the gyroscope of the form:

$$\begin{aligned} \mathbf{M}(d)\ddot{\mathbf{x}}(t) + \mathbf{D}(d,\theta)\dot{\mathbf{x}}(t) + \mathbf{K}(\theta) &= \mathbf{B}\mathbf{u}(t), \\ \mathbf{y}(t) &= \mathbf{C}\mathbf{x}(t), \end{aligned} \tag{29}$$

where $\mathbf{M}(d) = \mathbf{M}_1 + d\mathbf{M}_2 \in \mathbb{R}^n$, $\mathbf{D}(d,\theta) = \theta(\mathbf{D}_1 + d\mathbf{D}_2) \in \mathbb{R}^n$, $\mathbf{K}(d) = \mathbf{T}_1 + \frac{1}{d}\mathbf{T}_2 + d\mathbf{T}_3 \in \mathbb{R}^n$, $\mathbf{B} \in \mathbb{R}^n$, and $\mathbf{C}^\top \in \mathbb{R}^n$; $\mathbf{x}(t) \in \mathbb{R}^n$, $\mathbf{u}(t) \in \mathbb{R}^m$, and $\mathbf{u}(t) \in \mathbb{R}^q$ are the state, input and output vectors, respectively. Typical ranges for the parameters θ and d are $\left[10^{-5}, 10^{-7}\right]$ and $\left[1, 2\right]$, respectively. Finite-element discretization leads to $n = 17{,}913$. Normally, the system is operated in the frequency range $2\pi \cdot \left[0.025, 0.25\right]$. For more details on the model, we refer the reader to References 39,40.

In order to apply the proposed method, we take 500 points for frequency s in logarithmic scale and the same number of random points for the parameter $\mathbf{p} = \left[d, \theta\right]^\top$ in the considered range. In Figure 13, we first show the singular values, obtained by employing Algorithm 1, which indicates a rapid decay. Since the magnitude of the transfer function of the system is very small and wide ranged, $(10^{-7} - 10^{-3})$, we choose to truncate at a relatively low level. Hence, we truncate at 10^{-15}, thus leading to a reduced-order system of order $r = 80$. We compare the quality of the reduced-order system with the reduced-order system, obtained in Reference 35, where the authors have obtained a reduced-order system of order $r = 210$.

We compare the Bode plots of the original and reduced-order systems in Figure 11 for four different parameter settings and the Bode plots of the error systems are plotted in Figure 14. These figures indicate that both reduced-order systems are of very similar quality; but our reduced-order system is of order $r = 80$, whereas the method proposed in Reference 35 yields a reduced-order system of order $r = 210$, which is more than two-and-half times larger than ours.

6 | CONCLUSIONS

In this paper, we have studied model order reduction for linear structured parametric systems. Firstly, we recall the construction of an interpolatory reduced-order system for a given set of interpolation points. Then, we have defined the concepts of reachability and observability for linear structured parametric systems and connected them with interpolation-based MOR methods. Subsequently, by combining both features, we have discussed the construction of reduced-order systems by projecting onto those subspaces that are indicated by our approach as the most reachable and observable ones simultaneously. Moreover, we have shown the efficiency of the proposed methods by means of various examples, appearing in science and engineering.

The notion of minimal structured realizations opens several future directions, in particular, construction of minimal realizations via Petrov-Galerkin projection. For this, a full characterization of the concept of minimal realization for structured systems needs to be developed. One interesting future direction would be to combine the knowledge of error estimates, for example, from References 35,41 that allow to choose good interpolations points instead of just taking them randomly or in a logarithmic scale. Moreover, an extension to structured nonlinear systems by combining the ideas presented in this paper and in Reference 42 is a promising direction.

ACKNOWLEDGMENTS

We would like to thank Ali Seyfi for helping us with the implementation of numerical methods during his internship at the Max Planck Institute for Dynamics of Complex Technical Systems, Magdeburg, Germany. Moreover, we would like to express our gratitude to Dr Tobias Breiten and Dr Lihong Feng for providing the data from their publications. Open Access funding enabled and organized by Projekt DEAL.

DATA AVAILABILITY STATEMENT

The data that support the findings of this study are available from the corresponding author upon reasonable request.

ORCID

Peter Benner https://orcid.org/0000-0003-3362-4103
Pawan Goyal https://orcid.org/0000-0003-3072-7780
Igor Pontes Duff https://orcid.org/0000-0001-6433-6142

REFERENCES

1. Feng L, Benner P. Model order reduction for systems with non-rational transfer function arising in computational electromagnetics. In: Roos J, Costa LRJ, eds. *Scientific Computing in Electrical Engineering SCEE 2008*. Mathematics in Industry. Vol 14. Springer-Verlag; 2010:512-522.
2. Antoulas AC. *Approximation of Large-Scale Dynamical Systems*. SIAM Publications; 2005.
3. Benner P, Mehrmann V, Sorensen DC. *Dimension Reduction of Large-Scale Systems*. Lect. Notes Comput. Sci. Eng Vol 45. Springer-Verlag, Berlin/Heidelberg, Germany; 2005.
4. Benner P, Saak J. Efficient balancing-based MOR for large-scale second-order systems. *Math. Comput. Model. Dyn. Syst.* 2011;17(2):123-143. doi:10.1080/13873954.2010.540822
5. Chahlaoui Y, Lemonnier D, Vandendorpe A, Van Dooren P. Second-order balanced truncation. *Linear Algebra Appl.* 2006;415(2–3):373-384. doi:10.1016/j.laa.2004.03.032
6. Eid R, Salimbahrami B, Lohmann B, Rudnyi EB, Korvink JG. Parametric order reduction of proportionally damped second-order systems. *Sensors Mater*. 2007;19(3):149-164.
7. Reis T, Stykel T. Balanced truncation model reduction of second-order systems. *Math Comput Model Dyn Syst*. 2008;14(5):391-406.
8. Jarlebring E, Damm T, Michiels W. Model reduction of time-delay systems using position balancing and delay Lyapunov equations. *Math Control Signals Syst*. 2013;25(2):147-166.
9. Plischke E. *Transient Effects of Linear Dynamical Systems*. PhD thesis. Universität Bremen; 2005.
10. Benner P, Gugercin S, Willcox K. A survey of projection-based model reduction methods for parametric dynamical systems. *SIAM Rev*. 2015;57(4):483-531. doi:10.1137/130932715
11. Breiten T. Structure-preserving model reduction for integro-differential equations. *SIAM J Cont Optim*. 2016;54(6):2992-3015. doi:10.1137/15M1032296
12. Antoulas AC, Beattie CA, Gugercin S. Interpolatory model reduction of large-scale dynamical systems. In: Mohammadpour J, Grigoriadis KM, eds. *Efficient Modeling and Control of Large-Scale Systems*. Springer; 2010:3-58. doi:10.1007/978-1-4419-5757-3_1
13. Beattie CA, Gugercin S. Interpolatory projection methods for structure-preserving model reduction. *Syst Control Lett*. 2009;58(3):225-232. doi:10.1016/j.sysconle.2008.10.016
14. Schulze P, Unger B, Beattie C, Gugercin S. Data-driven structured realization. *Linear Algebra Appl.* 2018;537:250-286.
15. Hund M, Mitchell T, Mlinarić P, Saak J. Optimization-based parametric model order reduction via $\mathscr{H}_2\otimes_2$ first-order necessary conditions. *SIAM J. Sci. Comput.* 2022;44(3):A1554-A1578. doi:10.1137/21M140290X
16. Mayo AJ, Antoulas AC. A framework for the solution of the generalized realization problem. *Linear Algebra Appl.* 2007;425(2-3):634-662.
17. Baur U, Beattie CA, Benner P, Gugercin S. Interpolatory projection methods for parameterized model reduction. *SIAM J Sci Comput*. 2011;33(5):2489-2518.
18. Dullerud GE, Paganini F. *A Course in Robust Control Theory: a Convex Approach*. Vol 36. Springer Science & Business Media; 2013.
19. Anderson BDO, Antoulas AC. Rational interpolation and state-variable realizations. *Linear Algebra Appl*. 1990;137(138):479-509.
20. Fuhrmann PA. Exact controllability and observability and realization theory in Hilbert space. *J Math Anal Appl*. 1976;53(2):377-392.
21. Vidyasagar M. On the controllability of infinite-dimensional linear systems. *J Opt Th Appl*. 1970;6(2):171-173.
22. Curtain RF, Zwart H. *An Introduction to Infinite-Dimensional Linear Systems Theory*. Vol 21. Springer; 2012.
23. Kamen EW. Lectures on algebraic system theory: linear systems over rings. *Tech Rep NASA Contractor Report*. 1978:3016.
24. Kamen EW. Linear systems over rings: from R. E. Kalman to the present. *Math. System Theory*. Springer; 1991:311-324.
25. Lee E, Olbrot A. Observability and related structural results for linear hereditary systems. *Internat J Control*. 1981;34(6):1061-1078.
26. Morse AS. Ring models for delay-differential systems. *Automatica*. 1976;12(5):529-531.
27. Sontag E. Linear systems over commutative rings: a survey. *Ricerche di Automat*. 1976;7(1):1-34.
28. Gripenberg G, Londen S-O, Staffans O. *Volterra Integral and Functional Equations*. Vol 34. Cambridge University Press; 1990.
29. Weiss L. On the controllability of delay-differential systems. *SIAM J. Cont. Optim.* 1967;5(4):575-587.
30. Yi S, Nelson PW, Ulsoy AG. Controllability and observability of systems of linear delay differential equations via the matrix Lambert W function. *IEEE Trans Automat Contr*. 2008;53(3):854-860.
31. Gallivan K, Vandendorpe A, Van Dooren P. Model reduction of MIMO systems via tangential interpolation. *SIAM J Matrix Anal Appl*. 2004;26(2):328-349.
32. Georgieva I, Hofreither C. Greedy low-rank approximation in Tucker format of solutions of tensor linear systems. *J Comput Appl Math*. 2019;358:206-220.
33. Kressner D, Sirković P. Truncated low-rank methods for solving general linear matrix equations. *Numer Lin Alg Appl*. 2015;22(3):564-583.

34. Lee K, Elman HC, Powell CE, Lee D. Alternating energy minimization methods for multi-term matrix equations. arXiv preprint arXiv:2006.08531.
35. Feng L, Antoulas AC, Benner P. Some a posteriori error bounds for reduced order modelling of (non-)parametrized linear systems. *Esaim: M2AN*. 2017;51(6):2127-2158. doi:10.1051/m2an/2017014
36. Miller RW. *Flow Measurement Engineering Handbook*. McGraw-Hill; 1996.
37. The MORwiki Community. Anemometer, MORwiki–Model Order Reduction Wiki. 2018 http://modelreduction.org/index.php/Anemometer
38. Moosmann C, Rudnyi E, Greiner A, Korvink J, Hornung M. Parameter preserving model order reduction of a flow meter. *Proc Nanotech*. 2005;3:684-687.
39. Moosmann C. *ParaMOR - Model Order Reduction for Parameterized MEMS Applications*, PhD thesis. Albert-Ludwigs-Universität Freiburg; 2007 http://nbn-resolving.de/urn:nbn:de:bsz:25-opus-39719
40. The MORwiki Community. Modified gyroscope, MORwiki – Model Order Reduction Wiki. 2018 http://modelreduction.org/index.php/Modified_Gyroscope
41. Feng L, Benner P. On error estimation for reduced-order modeling of linear non-parametric and parametric systems. *ESAIM: Math Model Numer Anal*. 2021;55(2):561-594. doi:10.1051/m2an/2021001
42. Benner P, Goyal P. Interpolation-based model order reduction for polynomial systems. *SIAM J. Sci. Comput.* 2021;43(1):A84-A108. doi:10.1137/19M1259171

How to cite this article: Benner P, Goyal P, Pontes Duff I. Identification of dominant subspaces for model reduction of structured parametric systems. *Int J Numer Methods Eng*. 2024;125(15):e7496. doi: 10.1002/nme.7496